# The sleep-wake distribution contributes to the peripheral rhythms in PERIOD-2

Marieke M.B. Hoekstra[1,2*], Maxime Jan[1*], Yann Emmenegger[1], Paul Franken[1]

[1]Center for Integrative Genomics, University of Lausanne, Lausanne, Switzerland

[2] current address: UK Dementia Research Institute at Imperial College London, Division of Brain Sciences, London, United Kingdom

* share first authorship on this work

## Abstract

In the mouse, *Period-2* (*Per2*) expression in tissues peripheral to the suprachiasmatic nuclei (SCN) increases during sleep deprivation (SD) and when animals are predominantly awake spontaneously, suggesting that the circadian sleep-wake distribution directly contributes to the daily rhythms in *Per2*. We found support for this hypothesis by recording sleep-wake state alongside PER2 bioluminescence in freely behaving mice, demonstrating that PER2 increases during spontaneous waking and decreases during sleep. The temporary reinstatement of PER2 rhythmicity in behaviorally arrhythmic SCN-lesioned (SCNx) mice submitted to daily recurring SDs substantiates our hypothesis. Mathematical modelling revealed that PER2 dynamics can be described by a damped harmonic oscillator driven by two forces, a wake-driven and a SCN-independent circadian force. Our work underscores the notion that in peripheral tissues the clock gene circuitry integrates sleep-wake information and could thereby contribute to behavioral adaptability to respond to homeostatic requirements.

**Keywords**: circadian rhythm, sleep, waking, *Period-2*, bioluminescence, locomotor activity, modeling.

## Introduction

The sleep-wake distribution is coordinated by the interaction of a circadian and a homeostatic process (Daan et al., 1984). The biological substrates underlying the circadian process are relatively well understood: circadian overt behavior of mammals is generated by the suprachiasmatic nuclei (SCN) located in the hypothalamus (Hastings et al., 2018). At the molecular level, so called 'clock genes' interact through negative transcriptional/translational feedback loops (TTFLs), where the CLOCK/NPAS2:ARNTL (BMAL1) heterodimers drive the transcription of their target genes, among them the *Period* (*Per1,2*) and *Cryptochrome* (*Cry1,2*) genes. Subsequently, PER and CRY proteins assemble into repressor complexes that inhibit CLOCK/NPAS2:ARNTL-mediated transcription, thereby preventing their own transcription, with the resulting reduction of the repressor complex allowing for a new cycle to start. This feedback loop, present in almost each cell of the mammalian body, interacts with other molecular pathways, together ensuring a period of ~24hr (Hastings et al., 2018). The SCN synchronizes peripheral clock gene expression rhythms through its rhythmic behavioral, electrical, and humoral output generated across the day (Schibler et al., 2015).

Although the molecular basis of sleep homeostasis is not as well understood, accumulating evidence suggests that, perhaps surprisingly, clock genes are involved in this process (Franken, 2013). This is illustrated by the sleep-deprivation (SD) induced increase in the expression of the clock gene *Per2* in tissues peripheral to the SCN including the cerebral cortex, liver, and kidney (Curie et al., 2013, 2015; Franken et al., 2007; Maret et al., 2007), while SD does not affect the expression of clock genes in the SCN (Curie et al., 2015; Zhang et al., 2016). Moreover, the highest levels of peripheral *Per2* expression are reached after the time of day mice were awake most, suggesting that also during spontaneous periods of waking *Per2* expression accumulates. Accordingly, lesioning of the SCN, which eliminates the circadian sleep-wake distribution, attenuates the circadian amplitude of clock gene transcripts and proteins in peripheral tissues (Akhtar et al., 2002; Curie et al., 2015; Tahara et al., 2012). Altogether, these studies suggest that sleeping and waking are important contributors to clock gene expression, but dissecting the contribution of sleep-wake state from circadian time is challenging as time-spent-awake also affects circadian time.

By simultaneously recording electroencephalogram (EEG), electromyogram (EMG), locomotor activity and PER2-dependent bioluminescence signals in freely behaving mice, we established that the circadian sleep-wake distribution importantly contributes to the daily rhythmic changes in peripheral PER2 levels. To further test our hypothesis, we predicted that i) in behaviorally arrhythmic SCN-lesioned (SCNx) mice, daily recurring SDs mimicking a circadian sleep-wake distribution, will temporarily reinstate high amplitude PER2 bioluminescence rhythms and ii) in intact rhythmic animals, reducing the amplitude of the circadian sleep-wake distribution will

65 result in a reduced amplitude of PER2 rhythms. While daily SDs indeed enhanced PER2
66 amplitude in SCNx mice that was sustained after cessation of the SDs, the protocol used to
67 reduce the amplitude of the sleep-wake distribution was not as efficient as anticipated, and
68 accordingly did not reduce PER2 rhythm amplitude in all mice. To reconcile the sleep-wake
69 driven and circadian aspects of PER2 dynamics, we implemented a mathematical model in
70 which waking represents a force that sets in motion a harmonic oscillator describing PER2
71 dynamics. We conclude that the sleep-wake distribution under undisturbed conditions is an
72 important contributor to the daily changes in PER2 bioluminescence. Moreover, we discovered
73 a second, SCN and sleep-wake independent force with a circadian period that underlay the
74 residual circadian PER2 rhythms we observed in SCNx mice. The phase relationship between
75 these two forces is important for predicting the response in PER2 level to sleep-wake
76 perturbations.

77

78 **Results**

79 To quantify PER2 levels, we used mice expressing a knock-in (KI) construct encoding a fused
80 PER2::LUCIFERASE (PER2::LUC) protein and in which changes in emitted bioluminescence
81 can be used as proxy for changes in PER2 protein levels (Yoo et al., 2004). *Per2::Luc* KI mice
82 have been used to follow clock gene expression *in vivo* (Curie et al., 2015; Ohnishi et al., 2014;
83 Tahara et al., 2012; van der Vinne et al., 2018). However, in these studies mice had to be
84 anaesthetized for each measurement, while in the set-up used in our study [RT-Biolumicorder
85 (C. Saini et al., 2013)], we were able to assess PER2-bioluminenscence continuously in freely
86 moving mice. For all bioluminescence experiments, we used hairless SKH1 mice carrying the
87 *Per2::Luc* KI construct because lack of fur allows for the unobstructed measurement of emitted
88 photons. Under standard LD12:12 conditions, SKH1 mice exhibited sleep-wake patterns
89 characteristic of mice, i.e. during the light phase they spent more time in both Non-Rapid-Eye-
90 Movement (NREM) sleep and REM sleep relative to the dark phase, the latter being their
91 habitual active phase. Moreover, they showed the typical sleep homeostatic response to a 6h
92 SD during the first 18hrs of recovery, both in sleep time and EEG delta power, although the
93 increase in REM sleep did not reach significance levels (Suppl. Fig. 1).

94 In two pilot experiments we optimized our experimental set-up. We established that the most
95 important source contributing to the bioluminescence signals are the kidneys (Suppl. Fig. 2A).
96 Moreover, using mice constitutively expressing luciferase (Y.-A. Cao et al., 2004), we
97 determined that its substrate luciferin is best delivered through implantable osmotic mini-
98 pumps compared to administration through the drinking water. Under the latter condition,

99 strong daily rhythms in bioluminescence were observed, likely as a result of rhythms in drinking
100 behavior thereby driving luciferin availability (Suppl. Fig. 2B).

101

102 SLEEP-WAKE STATE AFFECTS PER2 BIOLUMINESCENCE

103 It now has been well documented that enforced wakefulness affects *Per2* mRNA and protein
104 levels in various tissues and mammalian species (Franken, 2013; Hoekstra et al., 2019; Möller-
105 Levet et al., 2013; Vassalli & Franken, 2017; Zhang et al., 2016), but it is not known whether
106 circadian rhythms in spontaneous sleep-wake behavior contribute to the daily changes in
107 PER2 levels. To address this question, we equipped SKH1 mice with wireless EEG/EMG
108 recorders and monitored simultaneously sleep-wake state, PER2 bioluminescence and
109 locomotor activity under constant darkness (DD). With this set-up, we reproduced the circadian
110 changes in PER2 bioluminescence as well as the response to a 6h SD in peripheral tissue
111 (Fig. 1) as described previously (Curie et al., 2015).

112 Although a circadian modulation of PER2 bioluminescence is evident (see Fig. 1B and Suppl.
113 Fig. 3), we also observed additional changes in bioluminescence that occurred simultaneously
114 with changes in sleep-wake state, indicating that PER2 bioluminescence increases during
115 wake-dominated periods and decreases during sleep-dominated periods. To quantify this
116 observation, transitions from sleep (irrespective of sleep state) to wake and from wake to sleep
117 were selected (see Material and Methods for selection criteria). We obtained 14.8±2.3
118 (mean±SEM, n=5) transitions from sleep to wake and 19.4±2.3 transitions from wake to sleep
119 during the two-and-a-half baseline days. Examples of selected transitions are indicated by the
120 hypnogram in Fig. 1B. Aligning these transitions revealed that a transition from wake to sleep
121 was accompanied with a 10% reduction (relative to levels at t=0; i.e., the transition) in
122 bioluminescence after 30 minutes (90.0±1.8%), whereas a transition from sleep to wake was
123 accompanied by a 25% increase in bioluminescence after 30 minutes (124.6±5.5%). Because
124 the changes at sleep-wake transitions in baseline demonstrate that waking is associated with
125 increases in PER2 bioluminescence and because animals are awake more in the active period
126 when PER2 is high, it altogether suggests that the sleep-wake distribution importantly
127 contributes to circadian changes in PER2.

128 Next, we assessed whether the sleep-wake evoked responses in peripheral PER2
129 bioluminescence depends on circadian phase by fitting a sinewave to each bioluminescence
130 trace. This sinewave was divided into a rising and a falling limb of the ongoing oscillation,
131 corresponding to ≈ ZT6–18 and ZT18-6 under LD12:12 conditions, respectively (Fig. 1C). We
132 found that sleep after the wake-to-sleep transition was associated with a faster decrease in
133 bioluminescence levels when transitions occurred during the falling limb (Fig. 1D). Such a time

course is consistent with our earlier observation that the sleep-wake dependent change in *Per2* mRNA levels is larger when its direction matches that of the ongoing *Per2* rhythm (Curie et al., 2013). Conceptually, this can be understood by assuming a sleep-wake driven harmonic oscillator model in which a force provided by being awake pushes either with or against the movement of the ongoing oscillation, during the rising or falling limb, respectively. With this concept in mind, we designed two further experiments to dissect the contribution of waking and circadian time to the observed rhythms in PER2 bioluminescence.

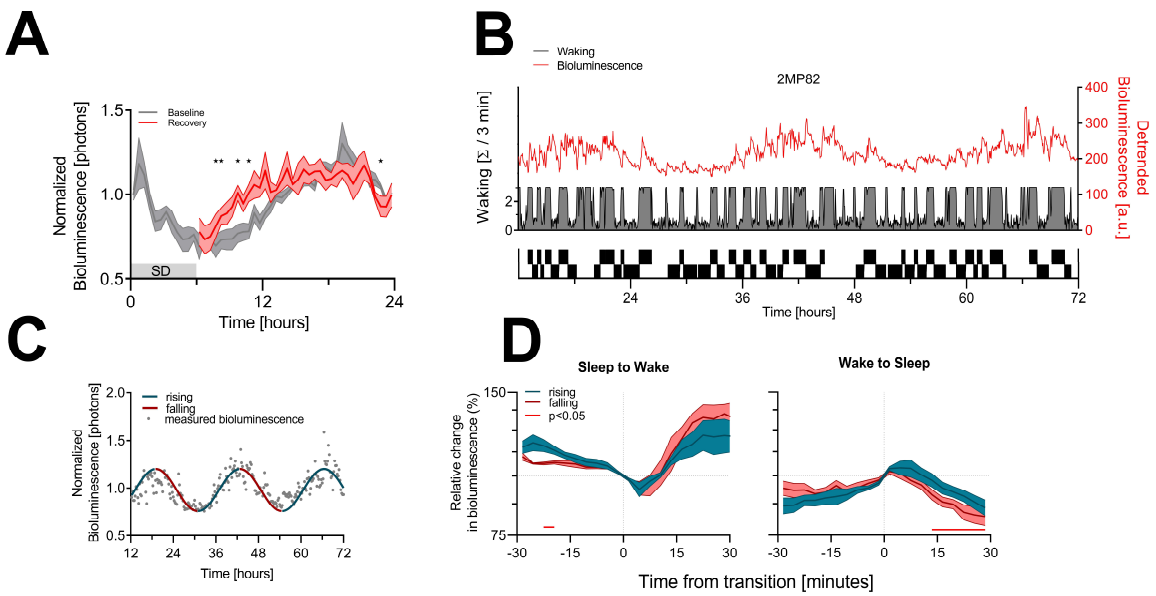


Figure 1: **The sleep-wake distribution contributes to changes in PER2 bioluminescence**. (**A**) Under baseline conditions (grey line), a clear circadian oscillation in PER2 bioluminescence was observed. Sleep depriving mice from, under preceding LD conditions, ZT0 to ZT6, affected PER2 bioluminescence during recovery (red; 2-way rANOVA w/ Condition x Time: $F(35,144)=2.1$, $p<0.001$, $n=5$). Asterisks indicate significant differences assessed by post-hoc paired t-tests. Bioluminescence is expressed as a fraction of the individual average bioluminescence during the experiment and depicted in 30min intervals as mean±SEM. (**B**) A sleep-wake state recording (grey area plot represents wakefulness in consecutive 3-min intervals) combined with peripheral PER2 bioluminescence (red line) in one individual mouse (ID# 2MP82). Note that besides the circadian oscillation in PER2 bioluminescence, there are marked increases and decreases in PER2 bioluminescence. The hypnogram (lower part of the graph) illustrates that the rapid evoked changes in PER2 bioluminescence are related to periods of sleeping (S) and waking (W). Note that this hypnogram is discontinuous as it depicts only the SW transitions selected in this mouse for the analysis in D. (**C**) A sinewave fitted to PER2 bioluminescence values

was used to delineate a rising (teal) and falling (red) limb. Data points reflect 15min mean bioluminescence levels. Data from the same mouse as in B. (**D**) Quantification of sleep-wake evoked changes in PER2 bioluminescence (mean±SEM). Sleep decreases whereas waking increases PER2 bioluminescence. The effect of sleeping and waking on changes in PER2 bioluminescence was modulated by circadian phase (rising vs. falling limb of the fitted sinewave; 2-way rANOVA, factor Time x Limb: sleep to wake $F(16,64)=3.5$, $p=0.0002$; wake to sleep: $F(19,76)=2.5$, $p=0.003$). The number of transitions did not differ between the rising and falling limb (Wilcoxon matched-pairs signed rank test; sleep to wake rising: 6.6±1.1; falling: 8.2±1.5, $p=0.50$; wake to sleep: rising: 11.0±1.4, falling: 8.4±1.9, $p=0.37$). Time in hours is depicted as ZT of the preceding day under LD12:12, y-axes tick marks are 12.5% $log_2$-scaled.

## MODULATING THE CIRCADIAN AMPLITUDE OF THE SLEEP-WAKE DISTRIBUTION AND ITS INFLUENCE ON PER2 BIOLUMINESCENCE

The SCN is the main driver of the circadian sleep-wake distribution because animals in which the SCN is lesioned (SCNx) lack a circadian organization of sleep-wake behavior under constant conditions (Baker et al., 2005; Edgar et al., 1993). Under these conditions, the amplitude of clock gene expression in peripheral organs is significantly reduced, but not eliminated (Akhtar et al., 2002; Curie et al., 2015; Kolbe et al., 2016; Tahara et al., 2012). Given our results in freely behaving mice, we expect that imposing a rhythmic sleep-wake distribution in SCNx mice will reinstate high-amplitude rhythmicity in PER2 bioluminescence. Conversely, reducing the amplitude of the circadian sleep-wake distribution in SCN-intact mice is expected to reduce the amplitude of PER2 bioluminescence. We tested these predictions in two complementary experiments. In the first experiment, we enforced a daily sleep-wake rhythm in arrhythmic SCNx mice by sleep depriving them for 4h at 24h intervals during 4 subsequent days. In the second experiment, we aimed to acutely reduce the circadian distribution of sleeping and waking in intact mice according to a ‘2hOnOff’ protocol, comprising of twelve 2h SDs each followed by a 2h sleep opportunity ‘window’ (SOW), previously utilized in the rat (Yasenkov & Deboer, 2010).

### *Repeated sleep deprivations in SCNx mice temporarily reinstate a circadian rhythm in PER2 bioluminescence*

Lesioning the SCN rendered locomotor activity arrhythmic under DD conditions (Suppl. Fig. 4). In arrhythmic SCNx mice we could confirm that rhythms in PER2 bioluminescence were strongly reduced, but not completely abolished (Fig. 2A and -B, Suppl. Fig. 5B and -C). During

165 the second baseline measurement after SCNx, we observed in 2 out of the 4 mice erratic high
166 values which we cannot readily explain (Fig. 2C), especially because in the subsequent four
167 SD days the variance in the PER2 bioluminescence signal among mice was again as small as
168 in the earlier recordings (Fig. 2A vs. -C). The repeated SDs induced a robust oscillation in the
169 PER2 bioluminescence signal that continued after the end of the SDs while decreasing in
170 amplitude (Fig. 2C).

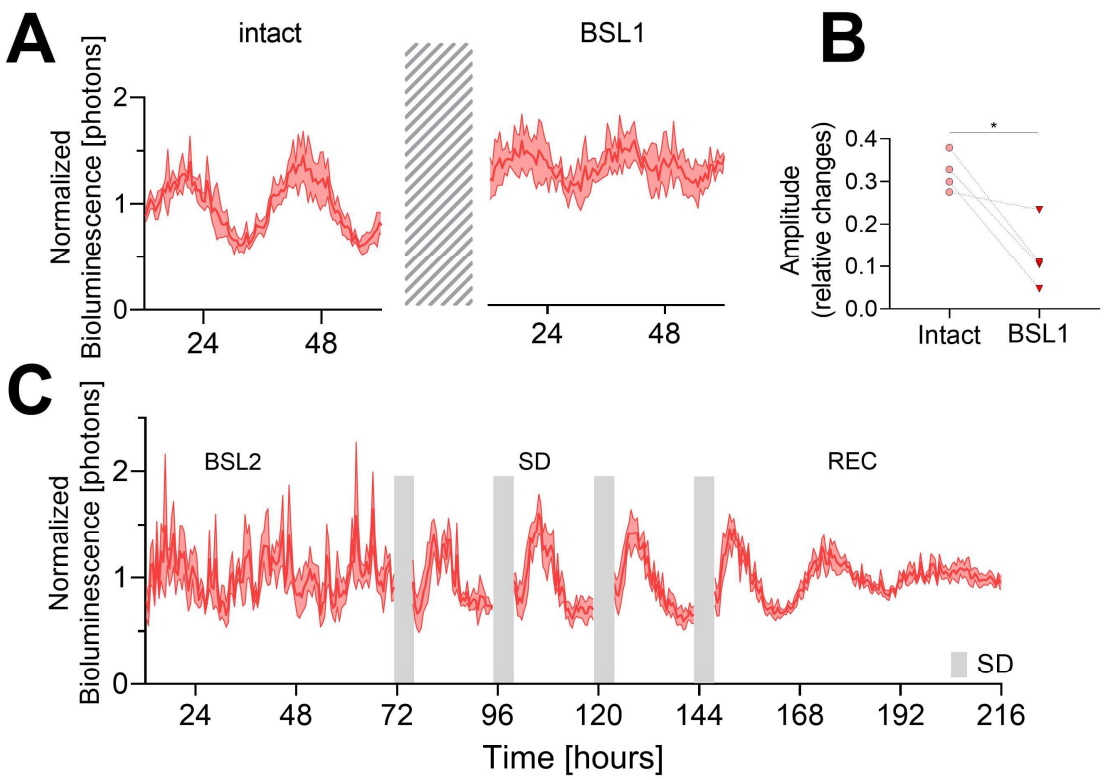


Figure 2: **Temporary reinstatement of circadian PER2 oscillations in SCNx mice by repeated sleep deprivations.** (**A**) Time course of PER2 bioluminescence across 2.5 days under baseline conditions (left) and after the SCN lesion (SCNx, right). Cross-hatched area represents approximately 5-week interval separating the 2 recordings during which the success of SCNx on locomotor activity was verified under DD (Suppl. Fig. 4). (**B**) SCNx reduced circadian PER2 bioluminescence amplitude (*, paired t-test, t(3)=3.7, p=0.03). (**C**) Four 4h sleep deprivations (SD, grey bars) repeated daily at the beginning of the under LD conditions, light phase, reinstate rhythmic PER2 bioluminescence (n=4). Abbreviation of experimental conditions: “intact”: baseline prior to SCNx; “SCNx-BSL1”: baseline after DD locomotor activity recordings; “SCNx-BSL2”: baseline immediately preceding the SDs; “SCNx-SD”: 20h recordings between the four 4h SDs; “SCNx-REC”: recovery after the four SDs. Data are depicted as mean±SEM (n=4).

171 *The 2hOnOff protocol reduced the amplitude of the circadian sleep-wake distribution without*
172 *impacting the circadian expression of PER2*

173 In the next experiment, we aimed at reducing the amplitude of the circadian sleep-wake
174 distribution in intact mice using the 2-day 2hOnOff protocol. We measured sleep-wake state
175 and PER2 bioluminescence during baseline conditions, the 2hOnOff procedure and the two
176 recovery days in two cohorts of mice. In the first cohort, PER2 bioluminescence was monitored
177 during the whole experiment, and mice were taken out of the RT-Biolumicorder for the 2h SDs
178 and therefore bioluminescence could only be quantified during the SOWs. A second cohort
179 was implanted with tethered EEG/EMG electrodes to determine the efficacy of the 2hOnOff
180 protocol in reducing the sleep-wake distribution amplitude in mice.

181 As expected, mice exhibited a circadian PER2-bioluminescence rhythm under baseline
182 conditions (Fig. 3A, 12-72hr and Fig. 3B). Contrary to expectation, the 2hOnOff protocol did
183 not noticeably affect the ongoing circadian PER2 oscillation (Fig. 3B), which was confirmed by
184 the quantification of the amplitude by sinewave fitting (Fig. 3C). Nevertheless, 4 out of 6 mice
185 did show a consistent 18% reduction in PER2-biolumininescence amplitude during the 2-day
186 2hOnOff protocol, while in the remaining two mice amplitude increased by 35% (Fig. 3C). In
187 all 6 mice, rhythm amplitude reverted to baseline values during recovery, irrespective of
188 whether it was increased or decreased during the 2hOnOff protocol.

189 In the second cohort we determined the extent by which the 2hOnOff protocol affected the
190 sleep-wake distribution. In contrast to bioluminescence, the amplitude of the circadian sleep-
191 wake distribution decreased in all mice (Fig. 3D and -E, right). The circadian rhythm in the
192 sleep-wake distribution was, however, not completely eliminated because of the sleep
193 obtained during the 2h SDs as well as during the 2h SOWs, which both varied as a function of
194 time of day (sleep during SDs: average: 12.4%, min-max: 4.9-23.0%; during SOWs: average:
195 54.3%, min-max: 35.7-76.4%). This was especially evident at the beginning of the subjective
196 light phase of day 2, where the average time spent asleep during the SD reached 23%. The
197 sleep obtained during the SDs at this time could be due to an substantial sleep loss during day
198 1 of the 2hOnOff protocol (total time spent asleep/day, mean±SEM; baseline: 11.1±0.1hr;
199 2hOnOff: day 1: 7.3±0.3hr, day 2: 8.6±0.7hr, paired two-tailed t-test, BSL versus 2hOnOff-day
200 1: $t(7)=8.86$, $p<0.001$; BSL versus 2hOnOff-day2: $t(7)=4.18$, $p=0.004$), 2hOnOff-day1 versus
201 day2, $t(7)=1.97$, $p=0.09$), combined with the difficulty for the experimenters to visually detect
202 and prevent sleep in pinkish hairless mice under dim-red light conditions. Although the daily
203 amplitude of the sleep-wake distribution was significantly reduced, this reduction appeared to
204 be insufficient to consistently reduce the amplitude of the PER2-bioluminescence oscillation in
205 all six mice.

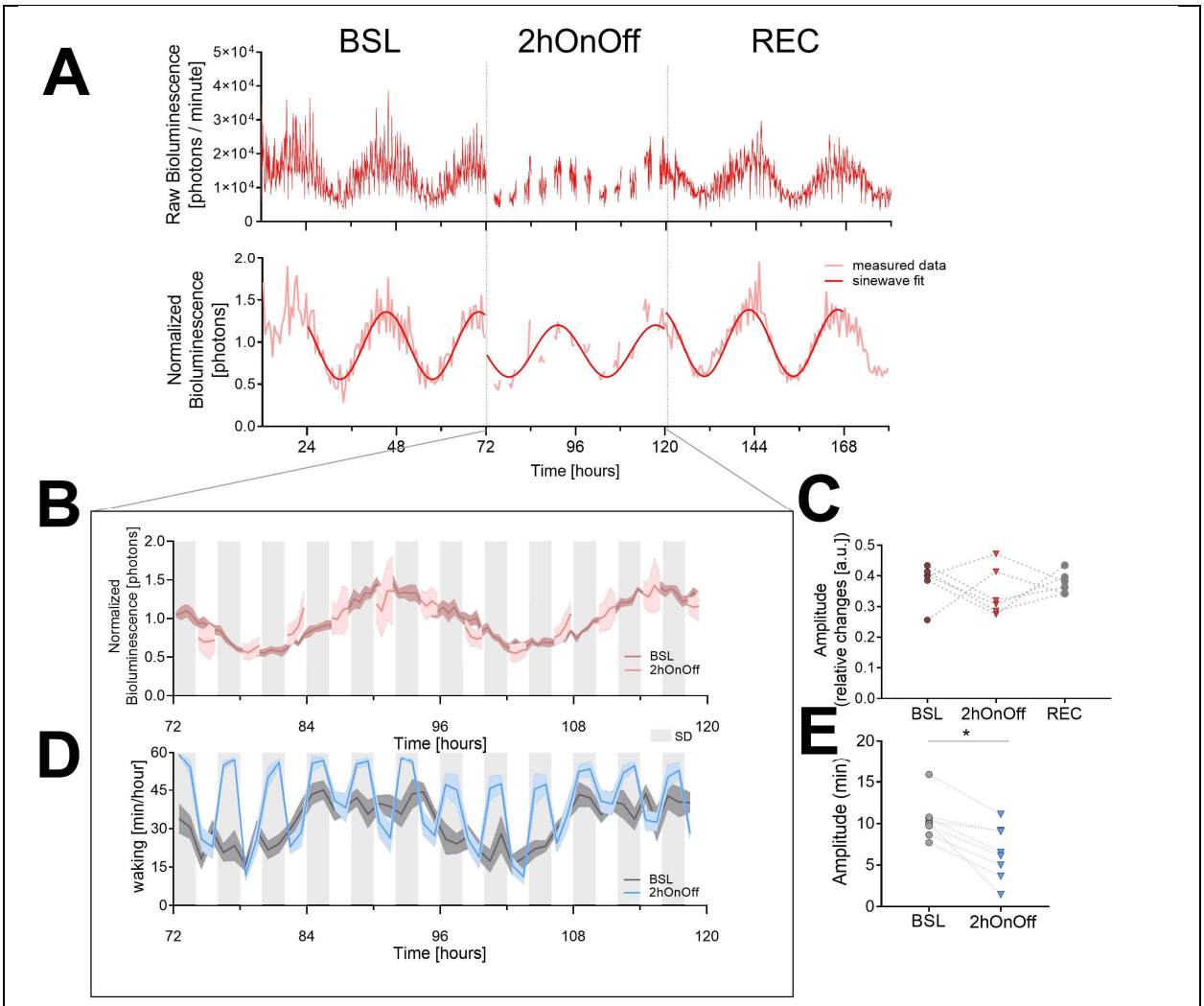


Figure 3: **The 2hOnOff protocol reduced the circadian sleep-wake amplitude but did not consistently affect PER2 bioluminescence. (A)** An example of a PER2-bioluminescence recording under baseline, 2hOnOff, and recovery conditions. Upper graph shows bioluminescence data as collected, whereas in the lower graph, the same data are linearly detrended, normalized (relative to the individual overall mean), and averaged over 30min intervals. A sinewave was fit to the data of the two baseline days, the two 2hOnOff days, and the two recovery days separately (see Materials and Methods). (**B**) The distribution of PER2 bioluminescence under baseline conditions and during the 2hOnOff protocol (n=6, data depicted as mean ± SEM). Light grey squares below the graph mark the 2h SDs (**C**) The amplitude of the PER2-bioluminescence rhythm decreased in 4 but increased in 2 mice resulting in overall lack of an effect of the 2hOnOff protocol (paired t-test, t(5)=0.74, p=0.50). For all 6 animals the amplitude reverted to baseline during recovery. (**D**) The distribution of waking across the two baseline days (dark grey) and during the 2hOnOff protocol (blue) in EEG-implanted SKH1 mice (n=8, hourly values depicted as mean ± SEM) and a sinewave fit through the hourly average for visual comparison of BSL to SD. (**E**) Individual estimates of the

amplitude of circadian changes in wakefulness during the 2hOnOff protocol were obtained by fitting a sine-wave function to the wakefulness present in consecutive 4h intervals (i.e. SD + SOW). This amplitude was smaller compared to the amplitude obtained in baseline using the same approach (paired t-test, t(7)=4.9, p=0.002). However, a circadian modulation was still present under the 2hOnOff protocol (amplitude>0, 1-sample t-test, t(7)=5.8, p=0.0007). The sleep-wake distribution during recovery was not assessed. Note the overall higher levels of wakefulness during 2hOnOff compared to baseline.

*Modeling circadian PER2 dynamics*

To put the observations of our last two experiments into a theoretical framework, we modeled changes in peripheral PER2 bioluminescence according to a driven harmonic oscillator. This type of oscillator is not self-sustained but depends on rhythmic forces to set in motion and maintain the oscillation. In the model we assume the sleep-wake distribution to represent such force. In the absence of rhythmic force(s), the oscillator loses energy resulting in a gradual reduction of its amplitude according to the rate set by its damping constant (γ). Besides amplitude and timing (i.e. phase) of the recurring forces and the damping constant, the oscillatory system is further defined by a string constant ($\omega_0^2$) determining its natural period. Because waking was not quantified alongside bioluminescence in the SCNx and the 2hOnOff experiment, we used locomotor activity (LMA), which correlates highly with time spent awake (Suppl. Fig. 5A, R2=0.79, p<0.0001), as a proxy for the driving force provided by wakefulness ($\vec{F}_{\mathrm{WAKE}}$). As a first assessment of the suitability of the model, we decided to perform the analyses at the group level; i.e., the mean LMA level of all mice was used to reflect $\vec{F}_{\mathrm{WAKE}}$, and the free parameters in the model were optimized by fitting the motion of the oscillator to the mean PER2 bioluminescence levels (see Material and Methods).

Besides $\vec{F}_{\mathrm{WAKE}}$, we needed to implement an additional circadian force to account for the residual PER2 bioluminescence rhythm observed in the SCNx mice (Suppl. Fig. 5B, -C, and Fig. 2). We assumed that this additional, SCN and sleep-wake independent force, reflects a peripheral circadian process ($\vec{F}_{\mathrm{PERI}}$) present in both intact and SCNx mice. This force was modeled as a sinewave with amplitude and phase as free parameters in both experiments while period was set to 23.7h which was the period estimated from the baseline PER2 bioluminescence rhythm observed in the SCNx mice (Suppl. Fig. 5C). A schematic overview of the influence of $\vec{F}_{\mathrm{PERI}}$ and $\vec{F}_{\mathrm{WAKE}}$ on PER2 bioluminescence is presented in Fig. 4A.

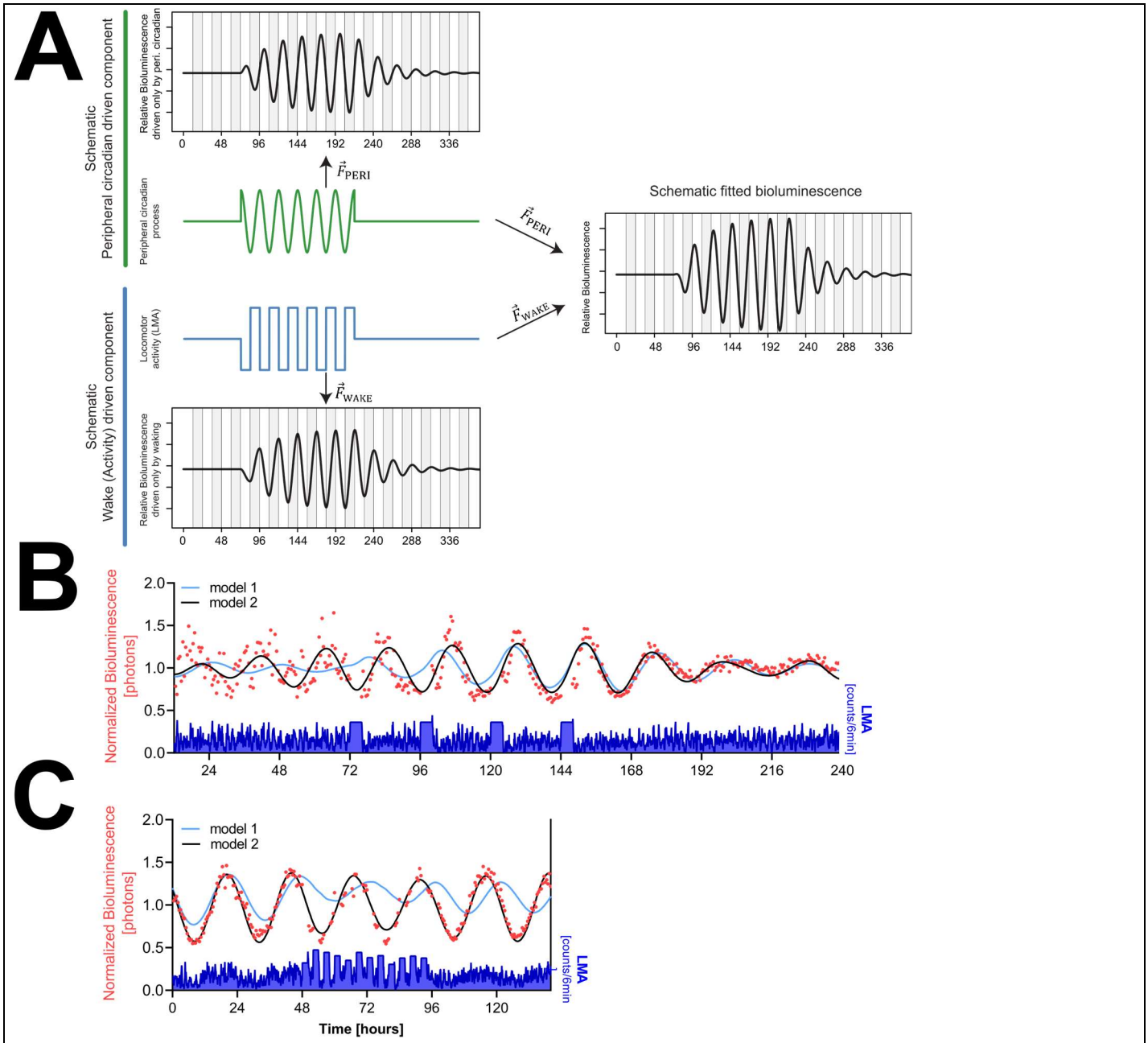


Figure 4: **Mathematical modeling of PER2 bioluminescence dynamics. (A)** Schematic view of a driven damped harmonic oscillator. The oscillation (black) is assumed be driven by two forces: $\vec{F}_{\mathrm{WAKE}}$ (blue) and $\vec{F}_{\mathrm{PERI}}$ (green). In our model $\vec{F}_{\mathrm{WAKE}}$ is based on LMA (here simplified as a square wave) and $\vec{F}_{\mathrm{PERI}}$ on a sinewave. Left panels show the individual effect of each force on the oscillator. Both forces start at t=72 h and end at t=216 h, illustrating the waxing and waning of the resulting rhythm amplitude. Right panel shows the resulting changes in PER2 bioluminescence when combining both forces. Note that combining the two forces increased amplitude and changed the phase of the oscillation. In this example, the amplitude of the peripheral circadian force is flat at beginning and end to illustrate that the oscillation is not self-sustained. **(B)** PER2 bioluminescence modeling in the SCNx experiment. LMA (lower graph in blue, 6min values) as the only driving force (model 1; blue line) or together with $\vec{F}_{\mathrm{PERI}}$ (model 2; black line) driving oscillations in PER2-bioluminescence (red dots, 30 minutes average). **(C)** Simulation of the PER2-biolumininescence in the 2hOnOff experiment using parameter estimates obtained in B (see Table 1). Details as in B.

232 We first optimized the performance of the model in predicting the PER2 bioluminescence
233 dynamics in the SCNx experiment (data from Fig. 2), and then evaluated the parameter
234 estimates by predicting the PER2 bioluminescence under the 2hOnOff experiment (data from
235 Fig. 3). With the optimized parameters listed in Table 1, the model accurately captured the
236 dynamic changes in PER2 bioluminescence in the SCNx experiment including the residual
237 rhythmicity in baseline, the reinstated pronounced rhythmicity during the 4 SDs, and its
238 subsequent dampening thereafter (Fig. 4B, black line). Using the same parameters, the model
239 also accurately predicted average bioluminescence dynamics in the 2hOnOff experiment (Fig.
240 4C, black line). It furthermore predicted an 18% reduction of PER2 bioluminescence amplitude
241 during the 2hOnOff protocol compared to baseline (relative amplitude 0.31 versus 0.38 [a.u.];
242 Fig. 4C), consistent with our hypotheses. The predicted reduction in amplitude matched
243 surprisingly well the 18% reduction in PER2 bioluminescence amplitude observed in the 4 mice
244 in which amplitude reduced (see Fig. 3C).

| Parameters | SCNx | 2hOnOff |
|---|---|---|
| γ (damping constant) | 0.0148 (0.0103 - 0.198) [$h^{-1}$] | |
| $\omega_0^2$ (string constant)) | 0.288 (0.285 - 0.291) [rad * $h^{-1}$] | |
| $\beta$ (coefficient $\vec{F}_{\mathrm{WAKE}}$ ) | 6.61e-5 (4.24e-5 - 8.90e-5) | |
| Model Intercept | 0.92 (0.901-0.515) | 0.90 (0.89 - 0.91) |
| $A$ (amplitude $\vec{F}_{\mathrm{PERI}}$) | 2.90e-3 (2.59e-3 - 3.31e-3) | 4.05-3 (3.9e-3 - 4.21e-3) |
| $\varphi$ (phase $\vec{F}_{\mathrm{PERI}}$) | 4.71 (4.6 - 4.81) | 2.74 (2.69 - 2.78) |

Table 1: **Parameter estimates obtained in the model optimization in the SCNx and 2hOnOff experiments**. Damping constant, natural frequency, and the $\vec{F}_{\mathrm{WAKE}}$ coefficient were optimized in the SCNx experiment and then used to predict the results of the 2hOnOff experiment. Amplitude and phase of $\vec{F}_{\mathrm{PERI}}$ were optimized for both experiments separately. The string constant determines the natural frequency of the harmonic oscillation with 0.288 rad * $h^{-1}$ corresponding to a period of 21.8h. Phase of the sine function describing $\vec{F}_{\mathrm{PERI}}$ is expressed as radians and corresponds to maximum values reached at time 11.9- and 19.4h for the SCNx and 2hOnOff experiment, respectively. Values in parenthesis represent the 95% confidence interval.

245

246 Next, we focused on the baseline days of the two experiments, allowing us to compare the
247 forces driving PER2 bioluminescence in animals with and without an intact SCN. The model
248 estimated that the mean total absolute force exerted on the relative PER2-bioluminescense
249 levels was more than twice as high during the baseline (t=0-48hr) in intact mice compared to
250 SCNx mice (2.69e-2 vs. 1.14e-2 h-2). This large difference was not due to differences in $\vec{F}_{\mathrm{WAKE}}$,

which was stable between the two experiments (2hOnOff vs. SCNx; 2.03e-3 vs. 2.20e-3 h-2), while $\vec{F}_{\mathrm{PERI}}$ was somewhat higher in intact mice (2.57e-3 vs. 1.86e-3 h-2). The higher mean total absolute force in intact mice could be attributed to increased string (2hOnOff vs. SCNx: 21.40e-3 vs. 7.05e-3 h-2) and damping forces (9.91e-4 vs. 3.14e-4 h-2) originating from a higher amplitude oscillation in intact mice (Suppl. Fig. 5B) and thus a larger PER2 'momentum' which is caused primarily by the presence of a circadian organization of wakefulness. This comparison also demonstrated that the direct effects of $\vec{F}_{\mathrm{WAKE}}$ and $\vec{F}_{\mathrm{PERI}}$ on PER2 bioluminescence do not depend on an intact SCN and that the contribution of the two forces are comparable.

Although without $\vec{F}_{\mathrm{PERI}}$ the model is unable to capture the residual PER2 rhythmicity in the baseline of the SCNx experiment (Fig. 4B, model 1 until 72hrs), removing $\vec{F}_{\mathrm{PERI}}$ from the model did not change the coefficient obtained for $\vec{F}_{\mathrm{WAKE}}$ (8.21e-5; 95%CI [6.6e-5 - 1.0e-4] compared to 6.61e-5 [4.2e-5 - 8.9e-5] in the full model). However, this simpler model (only 4 free parameters to estimate compared to 6 in the full model) could not accurately predict the bioluminescence data (Fig. 4B and -C; blue line) and fit statistics indicated a poorer fit (i.e., a higher BIC score, see Table 2). Moreover, by adding $\vec{F}_{\mathrm{PERI}}$, PER2 oscillations reached higher amplitude levels faster than without, contributing to the better fit of the rapid changes during the 4 SD days of the SCNx experiment, due to $\vec{F}_{\mathrm{PERI}}$ being in phase with the sleep deprivations. Together, these results highlight that both forces are needed to predict PER2 dynamics.

| | | **BIC** | **RSS** | **Bayes Factor** (model vs flat) |
|---|---|---|---|---|
| **SCNx** | $\vec{F} = \vec{F}_{\mathrm{WAKE}}$ | -291.39 | 11.98 | 1.07e32 |
| | $\vec{F} = \vec{F}_{\mathrm{WAKE}} + \vec{F}_{\mathrm{PERI}}$ | -432.4 | 8.38 | 4.53e62 |
| **2hOnOff** | $\vec{F} = \vec{F}_{\mathrm{WAKE}}$ | 18.99 | 14.97 | 1.58e6 |
| | $\vec{F} = \vec{F}_{\mathrm{WAKE}} + \vec{F}_{\mathrm{PERI}}$ | -538.9 | 1.31 | 2.22e127 |

Table 2: **Fitting statistics for the SCNx and 2hOnOff experiments using a single force** ($\vec{F}_{\mathrm{WAKE}}$) **or 2 forces** ($\vec{F}_{\mathrm{WAKE}}$ and $\vec{F}_{\mathrm{PERI}}$). Bayesian Information Criterion (BIC) for each model (lower is better; a BIC difference between two competing models larger than 10 is considered strong support for model with the lower value). Residual Sum of Square (RSS) minimized by the model (lower values reflect a better fit). Support of the driven harmonic model compared to a flat model using Bayes Factor (>100 is considered a 'decisive' support for the driven harmonic model). Values should be compared only within the same experiment because it depends on sample size which differed in the 2 experiments.

While the model accurately predicted overall PER2-bioluminescense dynamics in the 2hOnOff experiment, the amplitude reduction it predicted (and we anticipated) during the 2hOnOff intervention was not observed in the mean bioluminescence data. The individual data showed, however, that in 4 mice bioluminescence amplitude did diminish during the intervention as predicted while in the remaining 2 the opposite was observed (Fig. 3C). The model allows us to test in silico whether differences in initial conditions (such as phase and circadian period) could predict these opposite effects of the 2hOnOff intervention on PER2-bioluminecense amplitude. Surprisingly, we found that simply advancing the phase of $\vec{F}_{\mathrm{PERI}}$ by 6h during the baseline days prior to the 2hOnOff intervention resulted in an increase instead of decrease in PER2 amplitude during the 2hOnOff experiment (Suppl. Fig. 6A, dashed compared to solid lines). Phase differences among animals might relate to differences in the intrinsic circadian period length of their free-running rhythms under constant conditions that accumulate over time. We did not find a difference in PER2 bioluminescence or LMA phase at the end of the baseline recording (2.5 days under DD) between animals that decreased or increased PER2-bioluminescence amplitude. However, during the first day of recovery following the 2hOnOff protocol (5.5 days under DD), we observed a 2h phase advance in bioluminescence and 1h phase advance in LMA in the 2 mice that increased their amplitude during the preceding 2hOnOff protocol (Suppl. Fig. 6B, left), compared to the 4 mice for which we observed the anticipated decrease in PER2 amplitude (Suppl. Fig. 6B, right). Whether these differences in phase underlie the opposite response cannot be answered with the current data set. Nevertheless, the model yielded a perhaps counterintuitive but testable hypothesis by demonstrating that phase angle between the sleep-wake distribution and peripheral circadian clock-gene rhythms is an important variable in predicting outcome, as well emphasizes the importance of carefully controlling the initial conditions.

## Discussion

In this study we assessed the contribution of the sleep-wake distribution to circadian peripheral PER2 rhythmicity. We presented three key findings, supporting the notion that sleep-wake state is indeed an important factor in determining the circadian amplitude of peripheral changes in PER2: i) sustained bouts of waking and sleep were associated with increased and decreased PER2 bioluminescence, respectively; ii) repeated SDs temporarily reinstated robust rhythmicity in PER2 bioluminescence in behaviorally arrhythmic mice, and iii) mathematical modeling suggest that PER2 dynamics is best understood as an harmonic oscillator driven by two forces: a sleep-waking dependent force ($\vec{F}_{\mathrm{WAKE}}$) and a SCN-independent and sleep-wake independent, circadian peripheral force ($\vec{F}_{\mathrm{PERI}}$).

305

306 HOW DOES WAKEFULNESS INCREASE PER2?

307 *Per2* transcription can be initiated from its cognate E-boxes by CLOCK/NPAS2:ARNTL. This
308 transcriptional activation is at the core of the TTFL driving the circadian changes in PER2.
309 Enforced wakefulness not only affects *Per2* levels but also modulates the expression of other
310 components of the TTLF (Mang & Franken, 2015; Hor et al. 2019). The SD-evoked increase
311 in *Per2* expression could therefore be mediated through other clock genes in the circuitry as
312 was demonstrated in mice lacking the core clock genes *Npas2* and both *Cry1* and *-2* genes
313 (Franken et al., 2006; Wisor et al., 2002).

314 Apart from a TTFL-mediated activation, *Per2* transcription can be induced by other signaling
315 molecules directly acting on elements within the *Per2* promotor (Schibler et al., 2015). For
316 example, ligand-bound glucocorticoid receptors can induce *Per2* transcription by binding to
317 their glucocorticoid responsive elements (Cheon et al., 2013; So et al., 2009). Similarly, cAMP
318 response element (CRE)-binding protein (CREB), heat-shock factor 1 (HSF1), and serum-
319 response factor (SRF) can directly activate *Per2* transcription through CREs, heat-shock
320 elements, and CArG-boxes, respectively, present in the *Per2* gene (Gerber et al., 2013;
321 Camille Saini et al., 2012; Tamaru et al., 2011; Travnickova-Bendova et al., 2002). Through
322 these pathways, *Per2* responds to stress, light, temperature, blood-borne systemic cues, and
323 cellular activation as an immediate early gene (IEG). Because of this, *Per2* can appear
324 rhythmic even in the absence of a functional TTFL, provided these signaling pathways fluctuate
325 cyclically (Kornmann et al., 2007). In behaviorally arrhythmic SCNx animals the residual PER2
326 rhythms we observed might similarly results from SCN-independent corticosterone (Andrews,
327 1968) or body temperature (Satinoff & Prosser, 1988) rhythms. Alternatively, as TTFL-driven
328 PER2 rhythms persist in *ex vivo* tissues from SCNx mice (Yoo et al., 2004), residual PER2
329 rhythms could be generated and maintained locally in peripheral tissues *in vivo* as well.

330 Important for the current study is that several of the pathways known to directly influence *Per2*
331 expression are activated by either spontaneous and/or enforced waking [e.g., corticosterone
332 (Mongrain et al., 2010), temperature (Hoekstra et al., 2019), serum-response factor (Hor et al.,
333 2019), pCREB (Cirelli & Tononi, 2000)] and are therefore good candidates linking sleep-wake
334 state to changes in PER2. The observed changes in PER2-bioluminescence were rapid and
335 suggest that increases in protein can occur within 30 min of spontaneous wakefulness. Other
336 studies document that PER genes can indeed be rapidly transcribed and translated. For
337 instance, a light pulse given at CT14 leads within an hour to a two-fold increase in *Per2*
338 transcript in the SCN (Yan & Silver, 2002). One study reported an even larger increase in
339 hepatic *Per2* transcript levels within 1 hr after food presentation in fasted rats (Wu et al., 2010),

340 underscoring the ability of this transcript to rapidly adapt to homeostatic need. *Per2* translation
341 is not solely dependent on *de novo* transcription and, for example in the SCN, light was shown
342 to promote *Per2* translation (R. Cao et al., 2015), suggesting that transcription would not be
343 necessary to increase PER2 protein levels. Such mechanism could also underlie the very fast
344 (<30min) 1.5-fold increase in PER2 protein observed in fibroblasts after serum shock (R. Cao
345 et al., 2015). However, as *Per2* mRNA levels are usually closely coupled to translation rates
346 (Castelo-Szekely et al., 2017), *de novo* transcription is likely to be an important contributor to
347 the changes in PER2 bioluminescence that follow sleep-wake transitions.

348 The obvious next step is to determine which pathway(s) contributes to the wake-driven
349 changes in PER2 protein. We already established that the sleep-deprivation incurred increase
350 in *Per2* in the forebrain partly depended on glucocorticoids (Mongrain et al., 2010). Along those
351 lines, restoration of daily glucocorticoid rhythms in adrenalectomized rats reinstates PER2
352 rhythms in several extra-SCN brain areas (Segall & Amir, 2010). To determine the contribution
353 of the aforementioned wake-driven factors, a genetic screen could be deployed where one-by-
354 one the regulatory elements in the *Per2* promoter are mutated, and the effect of sleep-wake
355 driven *Per2* changes is assessed. This approach has already been taken for the GRE and
356 CRE elements in the *Per2* promoter to test their respective roles in circadian phase resetting
357 and integrating light information (Cheon et al., 2013; So et al., 2009; Travnickova-Bendova et
358 al., 2002).

359

360 INSIGHTS FROM THE MODEL

361 The model accurately captured the main features of the PER2 dynamics observed in both
362 experiments, thereby giving further credence to the notion that sleep-wake state importantly
363 contributes to the changes in PER2 observed in the periphery. Moreover, it demonstrated that
364 the large amplitude of the circadian PER2 rhythm in intact mice is likely the result of the
365 momentum gained in the harmonic oscillator through the daily recurring sleep-wake
366 distribution. This is conceptually different from a currently accepted scenario, in which direct
367 and indirect outputs from the SCN assure phase coherence of locally generated self-sustained
368 circadian rhythms (Schibler et al., 2015). According to this model, loss of amplitude observed
369 at the tissue level in SCNx mice is caused by phase dispersion of the continuing rhythms in
370 individual cells. Among the SCN outputs thought to convey phase coherence are feeding,
371 locomotor activity and changes in temperature. Because these outputs are all associated with
372 the animal being awake, it can be argued that in both models the circadian sleep-wake
373 distribution is key in keeping peripheral organs rhythmic.

374 The harmonic oscillator model further showed that, although important, the sleep-wake force
375 alone was not sufficient to accurately predict PER2 dynamics. In addition to account for the
376 residual PER2 rhythms observed in undisturbed SCNx mice, the SCN-independent and sleep-
377 wake-independent circadian force greatly improved the performance of the model in both
378 experiments. The synergistic effect of both forces ($\vec{F}_{\mathrm{PERI}}$ and $\vec{F}_{\mathrm{WAKE}}$) was needed to explain the
379 rapid response to the SDs observed in the SCNx experiment and also in maintaining robust
380 circadian rhythms during the SDs in the 2hOnOff experiment as illustrated in Fig. 4A and -B,
381 respectively. Furthermore, this synergistic effect greatly depended on the relative phase of the
382 two forces as we could illustrate *in silico* for the 2hOnOff experiment: a relative subtle change
383 in the phase of $\vec{F}_{\mathrm{PERI}}$ might underlie the increase (instead of the predicted decrease) in PER2
384 amplitude in 2 of the 6 mice recorded.

385 Which pathways set the phase of $\vec{F}_{\mathrm{PERI}}$ and whether it is truly independent of $\vec{F}_{\mathrm{WAKE}}$, as
386 assumed in the model, our current results cannot answer. In an earlier modeling attempt using
387 a similar approach in SCN-intact, light-dark entrained mice, we also required a second force
388 to correctly predict the phase of the observed rhythm in brain *Per2* expression (Curie et al.,
389 2013). In that publication we based the second force on the pattern of corticosterone
390 production sharply peaking at ZT11 just prior to the light-dark transition. The phase of $\vec{F}_{\mathrm{PERI}}$ in
391 the 2hOnOff experiment, which followed a more gradual, sine-wave function of which values
392 became positive shortly after ZT11 (extrapolated from the preceding LD cycle), seems
393 consistent with this. In the SCNx experiment, the phase of $\vec{F}_{\mathrm{PERI}}$ was positioned ~7h earlier
394 with a positive driving force starting at the end of each of the SDs. As SD is accompanied by
395 an increase in corticosterone (Mongrain et al., 2010), the phase of $\vec{F}_{\mathrm{PERI}}$ could be associated
396 with corticosterone signaling also in the SCNx experiment. Thus in intact mice, the SCN output
397 would dictate the phase of corticosterone production in the adrenals (and thus that of $\vec{F}_{\mathrm{PERI}}$),
398 while in SCNx mice the phase of the corticosterone rhythm can be reset by stressors such as
399 SD. As PER2 and *Per2* levels in the SCN seem insensitive to SD (Curie et al., 2015; Zhang et
400 al., 2016), this could explain why the phase of $\vec{F}_{\mathrm{PERI}}$ is maintained in sleep-deprived SCN-intact
401 mice. Moreover, *ex vivo* experiments demonstrated that the adrenal gland can generate bona-
402 fide circadian rhythms in corticosterone release independent of the SCN (Andrews, 1968;
403 Engeland et al., 2018; Kofuji et al., 2016), even though SCNx is generally thought to abolish
404 rhythms in circulating corticosterone levels (Moore & Eichler, 1972). While rhythmic
405 corticosterone release represents a plausible candidate contributing to $\vec{F}_{\mathrm{PERI}}$, especially
406 considering its role in synchronizing peripheral clocks (Balsalobre et al., 2000; Cuesta et al.,
407 2015; Dickmeis, 2009; Le Minh et al., 2001), our current results cannot rule out other sources
408 underlying or contributing to $\vec{F}_{\mathrm{PERI}}$. Above we argued that also wakefulness (i.e., $\vec{F}_{\mathrm{WAKE}}$ in the

model) could influence peripheral PER2 through corticosterone signaling, further complicating the issue. Indeed, adrenalectomy was found to reduce (but not abolish) the SD-induced increase in *Per2* expression in the forebrain (Mongrain et al., 2010). However, enforced but not spontaneous wakefulness is accompanied by increases in corticosterone and the model could predict PER2 dynamics without having to distinguish between the two types of waking. Therefore, other candidate signals among those listed above must be considered to understand the biological basis of $\vec{F}_{\mathrm{PERI}}$ and $\vec{F}_{\mathrm{WAKE}}$.

Model optimization yielded an unexpected short 21.8h period for the natural frequency of the PER2 oscillator, which, in addition, differed from the 23.7h period we set for $\vec{F}_{\mathrm{PERI}}$. While in the intact mice of the 2hOnOff experiment it is difficult to independently determine $\vec{F}_{\mathrm{PERI}}$'s period, we estimated a 23.7h period length for the residual PER2 rhythmicity observed during baseline in SCNx mice, which we assume is driven by $\vec{F}_{\mathrm{PERI}}$. In intact mice kept under constant conditions, SCN output drives behavioral sleep-wake rhythms and synchronizes peripheral clock-gene rhythms forcing the entire system to oscillate at the intrinsic period of the SCN. Similarly, in behaviorally arrhythmic SCNx mice, we assume that the period of the observed residual PER2 rhythm reflects that of the only remaining driver, $\vec{F}_{\mathrm{PERI}}$, as $\vec{F}_{\mathrm{WAKE}}$ is no longer rhythmic and direct effects of the SCN are absent. *Ex vivo* experiments showed that periods vary among tissues and do not depend on whether tissues were obtained from an intact or SCNx mouse (Cederroth et al., 2019; Yoo et al., 2004), pointing to tissue-specific TTFLs, which we assume to underlie the intrinsic rhythmicity of both $\vec{F}_{\mathrm{PERI}}$ and PER2 bioluminescence in our experiments. The difference in period length of $\vec{F}_{\mathrm{PERI}}$ and that of the intrinsic PER2 oscillator therefore suggests that $\vec{F}_{\mathrm{PERI}}$ is not of renal origin; i.e. the tissue which contributed most to the bioluminescence signal we recorded.

## DO CHANGES IN BIOLUMINESCENCE REFLECT CHANGES IN PER2 LEVELS?

The method we implemented to quantify PER2 protein levels presents advantages over previous methods used. It enabled us to acquire data at a time resolution to link changes in PER2 to sleep-wake state transitions in individual mice. Moreover, because of the within-subject experimental design, there is a substantial reduction in data variability and, as illustrated with the effects of individual phase on PER2 amplitude in the 2hOnOff experiment, we could assess the presence of individual differences in the initial conditions that might influence experimental outcome. Finally, the number of mice needed for these experiments has been greatly reduced while obtaining better quality data.

A limitation of this method is the assumption that changes in bioluminescence reflect changes in PER2 protein levels. Using western blot, we previously validated that changes in

444 bioluminescence during baseline and after a 6h SD indeed reflect changes in PER2 protein
445 (Curie et al., 2015). Nevertheless, substrate availability can importantly contribute to the signal
446 as demonstrated in the experiment in which we delivered luciferin in the drinking water. Even
447 the use of osmotic mini-pumps does not guarantee constant delivery, as its release rate is
448 temperature dependent (Alzet, manufacturer's notes) and bioluminescence's increase during
449 wakefulness might therefore result from the accompanying increase in temperature during this
450 state. Arguments against a possible temperature effect on bioluminescence changes comes
451 from a study in which, using the same osmotic mini-pumps, the expression of two clock genes
452 known to oscillate in anti-phase could be confirmed (Ono et al., 2015), which would not be
453 possible if temperature was the main determinant of bioluminescence. Moreover, we observed
454 that the circadian rhythms of subcutaneous temperature and bioluminescence are ca. 4hrs out
455 of phase (data not shown), supporting that the large circadian changes in bioluminescence are
456 not driven by changes in luciferin availability. Nevertheless, to fully exclude that potential rate-
457 limiting availability of luciferin contributed to the fast sleep-wake evoked changes in PER2, we
458 would require confirmation which other techniques sufficiently sensitive to quantify the small
459 but consistent protein changes after 30min of waking or sleep.

460

461 CONCLUSIONS

462 In this study, we used a unique combination of methods allowing us to collect high-resolution
463 data of sleep-wake state in conjunction with PER2 levels and found that the sleep-wake
464 distribution profoundly affects PER2 bioluminescence in the periphery. Such behavior-
465 dependent plasticity of the peripheral time-keeping machinery enables the organism to
466 respond to challenges as time restricted feeding experiments have demonstrated (Damiola et
467 al., 2000; Saini et al., 2013). Besides its importance in regulating feeding and energy
468 homeostasis (Bass & Takahashi, 2010), the clock circuitry also plays a prominent role in sleep
469 homeostasis (Franken 2013). PER2 seems perfectly suited as an integrator of sleep-wake
470 state and circadian time, because it is sensitive to a variety of sleep-wake driven signals. Our
471 model suggests that having a large amplitude rhythm protects from acute disturbances of sleep
472 as observed in the 2hOnOff experiment, while sleep depriving arrhythmic SCNx mice had
473 immediate and large effects on PER2. These rapid effects could only be achieved through the
474 synergistic effect of a second force that we found to be independent of the SCN and the sleep-
475 wake distribution. The coordination of the sleep-wake force and this second force in the model
476 was critical in predicting the effects of sleep-wake interventions on PER2. Research on the
477 nature of this second force would therefore be important to facilitate phase resetting and
478 normalize disrupted clock gene rhythms under conditions of jet lag and shift work,
479 complementing strategies aimed at altering the timing of the central pacemaker.

## Acknowledgements

We are greatly indebted to all who helped with the sleep deprivations: Lisa Härri, Charlotte Hor, and Jeffrey Hubbard, and especially to those who sacrificed their sleep during the graveyard shifts: Kostas Kompotis, Simone Mumbauer, Violeta Castelo-Szekely and Sonia Jimenez. We would also like to thank Sonia for her help with the sleep-wake annotation of EEG/EMG files.

## Material and Methods

MICE AND HOUSING CONDITIONS

To measure peripheral PER2 bioluminescence levels, the *Per2::Luc* KI construct, originally on a C57BL/6J background (Yoo et al., 2004), was brought onto a SKH1 background through backcrossing. We used SKH1 male heterozygous *Per2::Luc* KI mice in our experiments. Mice were kept under a 12 h-light/12 h-dark cycle with light- and dark-onset referred to as Zeitgeber time (ZT)-0 and -12, respectively. Food and water was available *ad libitum,* and after surgery mice were singly housed. All experiments were approved by the Ethical Committee of the State of Vaud Veterinary Office Switzerland under license VD2743 and 3201.

SOURCE OF BIOLUMINESCENCE AND LUCIFERIN'S ROUTE OF ADMINISTRATION

Because *Per2::Luc* KI mice express ubiquitously luciferase and the RT-Biolumicorder cannot discriminate between different sources of bioluminescence, we assessed which peripheral organ(s) was/were the major source of bioluminescence. Two male heterozygous *Per2::Luc* SKH1 mice were implanted with an osmotic mini-pump (model 1002; 35mg/mL luciferin) and five days later lightly anaesthetized with 2.5% isoflurane and imaged for 60 seconds (Xenogen IVIS Lumina II) around ZT6. The main source of dorsal bioluminescence overlapped with the expected location of the kidney, whereas ventrally almost no bioluminescence was detected (see Suppl. Fig. 2). Most bioluminescence quantified during the experiment is of dorsal origin due to the orientation of the mouse relative to the PMT, suggesting that the kidneys are the main source of peripheral bioluminescence in *Per2::Luc* SKH1 mice. In a second pilot experiment, we investigated the optimal route of luciferin administration. Although luciferin administration via drinking water has been used before to measure bioluminescence (Saini et al., 2013, Iwano et al., 2018 SCIENCE, Hall et al., 2018 Nature Comm), we were concerned that this route could limit luciferin availability in a circadian fashion because drinking behavior has a strong circadian rhythm (Bainier, Mateo, Felder-Schmittbuhl, & Mendoza, 2017). To address these concerns, we made use of mice expressing constitutively luciferase under control of the synthetic CAG promotor [(Y. A. Cao et al., 2004), Jackson catalog number 008450], thus allowing for testing of circadian fluctuating levels of luciferin. Mice received luciferin via the drinking water or via an osmotic mini-pump and served as their own control. Four male CAG mice were housed for two subsequent experiments in constant darkness in the RT-Biolumicorder. During the first experiment, 0.5 mg/mL luciferin was dissolved in the drinking water. At the end of this experiment, mice received subcutaneously an osmotic mini-pump (Alzet, model 1002) under light anesthesia (isoflurane; 2-4% mixed with O2) containing 70 mg/mL of luciferin and could recover for two days, before bioluminescence and activity was monitored for the second experiment in the RT-Biolumicorder.

525

526 SURGICAL PROCEDURES AND EXPERIMENTAL DESIGN

527 *Sleep-wake state determination in parallel with PER2 bioluminescence*

528 Mice were implanted with electroencephalogram (EEG) and electromyogram (EMG)
529 electrodes under deep ketamine/xylazine anesthesia. Three gold-plated screws (frontal,
530 parietal and cerebellar) were screwed into the skull over the right cerebral hemisphere. Two
531 additional screws were used as anchor screws. For the EMG, a gold wire was inserted into the
532 neck musculature along the back of the skull. The EMG and three EEGs electrodes were
533 subsequently soldered to a connector and cemented to the skull. The cerebellar screw served
534 as a reference for the parietal and frontal screw and the EMG. After the first recovery day, mice
535 were habituated to the weight of the wireless EEG recording system by attaching a dummy of
536 same size and weight to their connector. Two days before habituation to the RT-Biolumicorder,
537 mice were implanted with the osmotic mini-pump (model 1002, Alzet; luciferin 35mg/mL) under
538 light anesthesia. 8-10 days post-surgery, mice were placed in the RT-Biolumicorder at the end
539 of the light phase (~ZT10-ZT12) for two days in LD to habituate to the novel environment. At
540 the end of the second habituation day, the dummy was replaced with a wireless EEG
541 (Neurologger, TSE Systems GmbH). After two-and-a-half days of baseline recording in
542 constant darkness, mice were sleep deprived for six hours at a time they were expected to rest
543 (ZT0 under LD conditions) by gentle handling as described (Mang & Franken, 2012). After SD,
544 mice were placed back into the RT-Biolumicorder for the subsequent two recovery days.

545 *Surgeries for tethered EEG/EMG recordings*

546 SKH1 mice (n=8) were implanted with EEG and EMG electrodes as described previously
547 (Mang & Franken, 2012) to determine sleep-wake state. The surgery took place under deep
548 xylazine/ ketamine anesthesia. Briefly, six gold-plated screws (diameter 1.1 mm) were screwed
549 bilaterally into the skull over the frontal and parietal cortices. Two screws served as EEG
550 electrodes and the remaining four screws anchored the electrode connector assembly. As
551 EMG electrodes, two gold wires were inserted into the neck musculature. The EEG and EMG
552 electrodes were soldered to a connector and cemented to the skull. Mice recovered from
553 surgery during several days before they were connected to the recording cables in their home
554 cage for habituation to the cable and their environment, which was at least 6 days prior to the
555 experiment. The habituation to the room and the recovery from the two-day SD-procedure took
556 place under LD 12:12 conditions.

557 During the baseline recording and sleep deprivation days, red light at very low intensity was
558 present to allow the experimenters to observe the mice. Mice were sleep deprived for two
559 hours according to the ‘gentle handling’ method (Mang & Franken, 2012).

560 *Mice for bioluminescence data collection*

561 SKH1 mice (n=6) were implanted with an osmotic mini-pump (Alzet, 1002, luciferin
562 concentration: 35 mg/mL; blue flow moderator) two days before the habituation. At the end of
563 the light phase (~ZT10-ZT12), mice were moved from their cage to the RT-Biolumicorder for
564 2-3 days of habituation in LD. They were housed for 2.5 days in DD, after which the 2hOnOff
565 protocol was initiated at light onset (ZT0) under the preceding LD conditions. At the start of
566 each SD, mice were moved from the RT-Biolumicorder and placed into a novel cage that was
567 in the same room as the EEG-implanted mice. Fifteen minutes before the end of each SD,
568 mice were brought back to their RT-Biolumicorder cage.

569

570 *SCNx experiment*

571 Four SKH1 mice were recorded over the course of the experiment and served as their own
572 control (see also Fig. 4A). Briefly, their PER2 bioluminescence rhythm was monitored before
573 SCNx (once), under undisturbed conditions post-SCNx (twice), and after the second measure
574 under SCNx conditions, the mice were subjected to the repeated 4hr SDs.

575 Bilateral lesion of the two SCNs was performed stereotaxically (Kopf Instruments, 963LS,
576 Miami Lakes, FL, USA) under ketamine/xylazine anesthesia (intraperitoneal injection, 75 and
577 10 mg/kg, at a volume of 8 mL/kg). Two electrodes (0.3 mm in diameter) were introduced
578 bilaterally at the following coordinates (anteroposterior using bregma as reference: ± 0.2mm
579 lateral, +0.5mm bregma, depth: -5.9mm). Electrolytic lesions (1 mA, 5 sec) were made using
580 a direct current (DC) lesion device (3500, Ugo Basile, Comerio, Italy). After lesion, mice stayed
581 3–4 days under LD12:12, followed by constant dark (DD) conditions for at least 10 days to
582 verify presence or absence of circadian organization of overt behavior. Activity was quantified
583 using passive infrared sensors (Visonic SPY 4/ RTE-A, Riverside, CA, USA). ClockLab
584 software (Actimetrics, Wilmette, IL, USA) was used for data acquisition and analyses.

585

586 DATA COLLECTION OF SLEEP-WAKE STATE

587 *Simultaneous recording of sleep-wake state and PER2 bioluminescence*

588 Batteries (Hearing Aid; Ansmann, 312 PR41, 1.45 V 180 mAh) were inserted into the
589 Neurologger. This insertion was timed with the clock of the computer that controlled the RT-
590 Biolumicorder to *post hoc* align the EEG/EMG signals with the bioluminescence signal. In
591 addition, time stamps provided by the SyncBox (NeuroLogger, TSE) were used to verify the
592 start and end time of the EEG/EMG recording. The cerebellar electrode was used as a
593 reference for both EMG and EEG. Data was sampled at 256 Hz. The frontal signal was
594 subtracted from the parietal signal (EDF Browser) to support sleep-wake state determination

595 by enhancing the identification of slow waves and theta waves within the same trace. The data
596 was subsequently loaded in Somnologica (Somnologica 3, MedCare) to determine offline the
597 mouse's behavior as wakefulness, REM sleep or NREM sleep per 4-second epochs based on
598 the EEG and EMG signals. Wakefulness was characterized by EEG activity of mixed frequency
599 and low amplitude, and present but variable muscle tone. NREM sleep (NREM) was defined
600 by synchronous activity in the delta frequency (1–4 Hz) and low and stable muscle tone. REM
601 sleep (REM) was characterized by regular theta oscillations (6–9 Hz) and EMG muscle atonia.

602

603 *2hOnOff experiment*

604 EEG and EMG signals were recorded continuously for 96 h. The recording started at the
605 beginning of the subjective rest phase, ZT0 of the preceding LD cycle. The analog EEG and
606 EMG signals were amplified (2,000×) and digitized at 2 kHz and subsequently down sampled
607 to 200 Hz and stored. Like the EEG and EMG traces obtained with the Neurologger, the data
608 was imported in SomnoLogica and sleep-wake state was determined per 4-second epochs.
609 LMA was monitored with passive infrared activity (ActiMetrics, US, Wilmette) and recorded
610 with ClockLab (ActiMetrics, US, Wilmette).

611

612 DATA ANALYSIS

613 *Route of luciferin administration*

614 Circadian time was determined to inspect the circadian changes in bioluminescence relative
615 to locomotor activity. To this end, the period length per mouse was determined based on
616 activity measurements (1-min resolution) by chi-square analysis in ClockLab. Subsequently,
617 the activity and bioluminescence data were folded according to the period. The activity data
618 was averaged per 10 minutes and activity onset was visually determined for each mouse and
619 set at CT12. The aligned activity and bioluminescence data were subsequently averaged per
620 circadian hour.

621

622 *Spontaneous sleep wake state and bioluminescence*

623 Bioluminescence and activity were sampled at a resolution of 4-seconds, which is the same
624 resolution of the epochs for sleep-wake state determination. Data processing was
625 subsequently performed in MatLab 2017b (The MathWorks, Inc., Natick, Massachusetts,
626 United States). Linear trends were removed from the signal by the build in function 'detrend'.
627 Subsequently, the bioluminescence signal was expressed relative to the overall mean per
628 mouse to account for interindividual differences. Changes in PER2 would be expected to occur

at a slower rate then 4-seconds. Therefore, sleep-wake and bioluminescence data are averaged per blocks of 3 minutes.

Selected sleep-wake transitions had to fit the following criteria: they had to last for at least 15 minutes before and after the transition, and time spent in sleep or wake bouts should be at least 50% in that designated state. With this selection criteria, we found periods of wakefulness and sleep. Bioluminescence levels at transitions were first averaged within mice and then across mice. A sinewave was fit through the bioluminescence data (averaged per 15 min) to determine occurrence of transitions on either the rising or falling limb (MatLab, $fit = Y_0 + a * \sin(\frac{2*pi}{b} + c)$).

*2hOnOff experiment*

Bioluminescence data obtained five minutes before and ten minutes after the sleep deprivations was excluded from analysis. Subsequent data normalization of the bioluminescence data was as above. To determine the influence of the 2hOnOff protocol on the strength of the ongoing circadian oscillation of the circadian distribution of sleep and wake, as well on PER2 bioluminescence, an estimation of amplitude by sinewave fitting was done (MatLab, $fit = Y_0 + a * \sin(\frac{2*pi}{b} + c)$).

*Modeling PER2 bioluminescence with a damped harmonic oscillator*

The temporal dynamic of PER2 bioluminescence was modeled according to the equation of motion describing a driven damped harmonic oscillator:

$$\frac{d^2x}{dt^2} + \gamma\frac{dx}{dt} + \omega_0^2 x = F$$

where x is the displacement of the oscillator, γ is the damping constant of the model and $\omega_0^2$ the natural frequency of the model. The driving forces used in this model are the locomotor activity (LMA) representing waking $\vec{F}_{\mathrm{WAKE}}$, and a second, circadian force $\vec{F}_{\mathrm{PERI}}$, represented as a sinewave. The force exerted on the oscillator is represented as the addition of these two forces (see Fig. 4):

$$F(t) = \beta LMA_t + A\sin(\omega t + \varphi)$$

Where $\beta$, $A$ and $\varphi$ are respectively the coefficient applied on locomotor activity amount, the amplitude of the circadian sinewave force and the phase of the circadian sinewave force. These coefficients were the free parameters to be optimized in the model. $\omega$ is the angular velocity of the sinewave and was set to 2*pi/23.7, based on the residual PER2-bioluminescence rhythm present in the baseline of SCNx mice. To solve this equation and optimize for parameters that best describe the observed PER2 bioluminescence, we proceeded as follows: The relative bioluminescence data from both experiments was averaged across mice using 30-minute bins. LMA was averaged across mice using 6-minute bins. Locomotor activity could not be measured directly during sleep deprivations (SD) and was estimated by assessing the increase in LMA during SDs measured in EEG-implanted mice, which was found to be 2.4 times higher compared to average baseline levels. Thus, the SD effect was estimated using 2.4 times the mean activity observed during baseline (i.e. 180.85 and 180.18 for the SCNx and 2hOnOff respectively).

To solve the 2nd order ordinary differential equation (ODE) of the driven harmonic oscillator, we transformed it into the following system of two first order ODEs describing the change of position and speed of our oscillator:

$$x'_1 = x_2$$

$$x'_2 = F - \gamma\, x_2 - \omega_0^2\, x_1$$

We then used the 4th order Runge-Kutta (RK4) numerical method to approximate the solution using a fixed time step of 0.1 hour. In the SCNx experiment, initial values of speed ($x_2(0)$) and position ($x_1(0)$) were set to 0. For the 2hOnOff experiment the model was generated for 20 days prior experiment to reach a steady-state using replication of LMA observed in baseline (T0-T24). The position and speed of the oscillator at the end of the 20 days were taken as initial values for the fitting. We optimized the model for the following parameters: intercept (equilibrium position of the oscillator), natural frequency, damping constant, and coefficient for the force exerted by LMA, amplitude of circadian force and phase of circadian force. We optimized the fitting minimizing the Residual Sum of Square (RSS) between predicted position of our model and the observed PER2 bioluminescence level. The box-constrained PORT routines method (nlminb) implemented in the optimx/R package (http://dx.doi.org/10.18637/jss.v043.i09) was used to minimize the RSS.

The goodness of fit of the model was assessed as follows. We assumed that the model errors follow a normal distribution and computed a Bayesian Information Criterion (BIC) value for the model according to:

$$BIC = n \ln\left(\frac{RSS}{n}\right) + k \ln(n)$$

Where n is the number of observations, and k is the number of parameters of the model. We approximated the Bayes Factor (BF) between our model and a flat model (linear model with intercept only) as follow:

$$BF \approx \exp\left(-\frac{1}{2}\left(BIC_{flat} - BIC_{model}\right)\right)$$

To compute confidence interval of our model parameters we used 500 Monte-Carlo simulations and calculated a confidence interval for our parameters based on 95% empirical quantiles. The method was adapted from the code of Marc Lavielle [Inria Saclay (Xpop) and Ecole Polytechnique (CMAP), Université Paris-Saclay, France] for nonlinear model available here: http://sia.webpopix.org/nonlinearRegression.html

*Statistics*

Statistics were performed in R (version 3.3.2) and Prism (version 7.0), with the threshold of significance set at α=0.05. Performed statistical tests are mentioned in the text and figure legends of the result section.

## Supplementary Figures

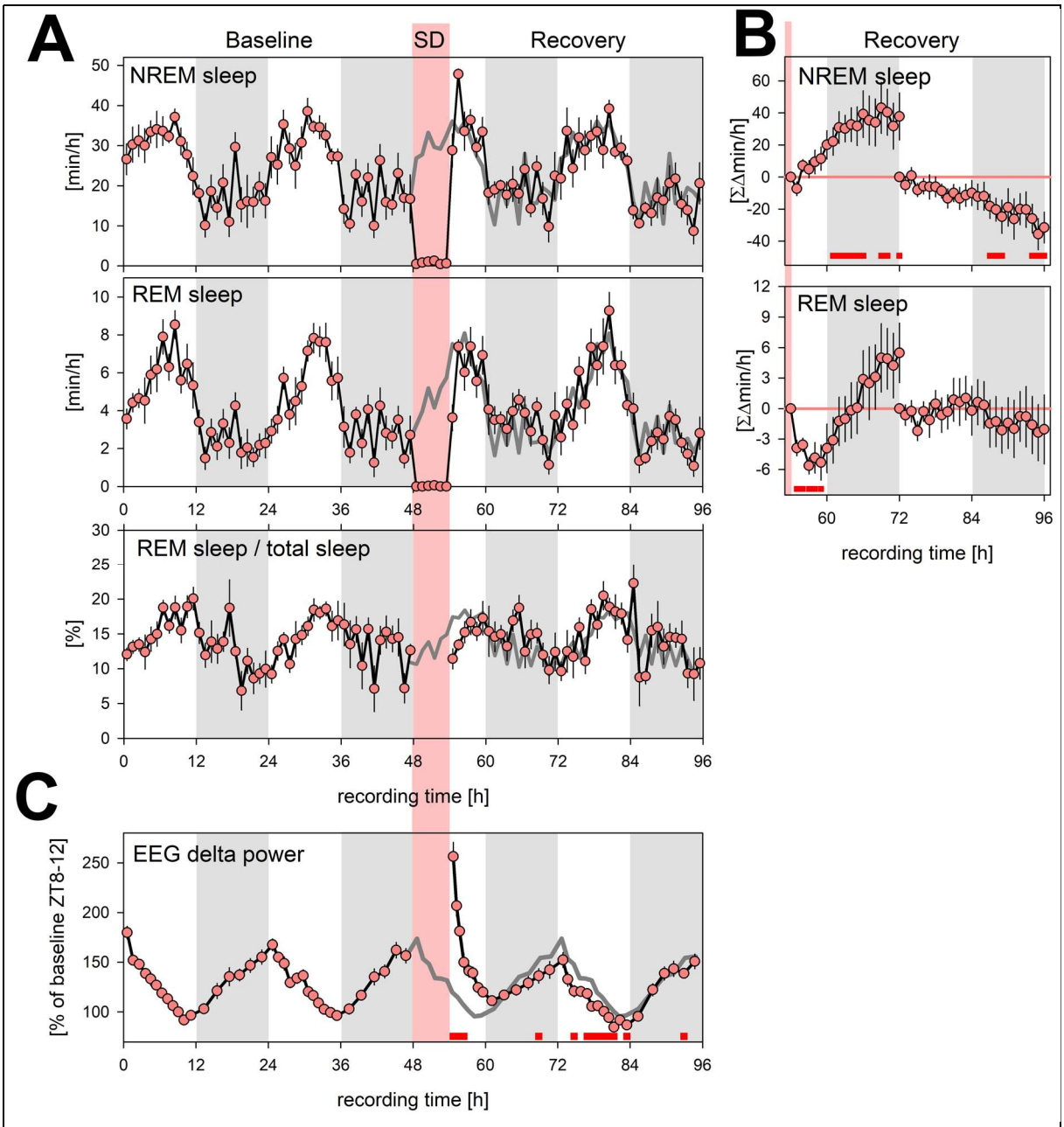


Supplementary Figure 1: **Sleep phenotyping of SKH1 mice.** Four-day time course of time spent asleep and EEG delta power (1-4Hz) during baseline, 6h sleep deprivation (SD; ZT0-6, t=48-54h; pink area), and recovery in SKH1 mice (n=8) under LD12:12 (grey areas denote the 12h D-periods) conditions. **(A)** NREM sleep (top) and REM sleep (bottom) as mean minutes over hourly intervals (±1 SEM). Dark grey line during SD and recovery represent baseline time course (mean over the 2 baseline days) for comparison. **(B)** Accumulated differences (min/h) from baseline separately for recovery day 1 (t=54-72h) and day 2 (t=72-96h). During recovery day 1 mice accrue ca. +38.8±14.6 min NREM sleep, which is again lost during recovery day 2 (-31.5±9.6 min). Mice lose -5.3±1.7 min of REM sleep during first

5 recovery hours after SD. This additional deficit is offset during the remaining of recovery day 1 resulting in a non-significant increase of 5.5±2.9 min. (**C**) Mean EEG delta power during NREM sleep (±1 SEM) calculated for 12 and 6 percentiles during the L- and D-periods, respectively (except for L-period recovery day 1; 8 percentiles) to which an equal number of 4s-epochs scored as NREM sleep contributed (per LD period and mouse). Delta power is considered an EEG correlate of sleep need decreasing when sleep prevails (L-period) and increasing when animals are mostly awake (D-periods). SD results in high immediate values that quickly revert to baseline. Red squares underneath curves represent hourly intervals in which values differed from baseline, post-hoc paired t-tests $p<0.05$.

723

724

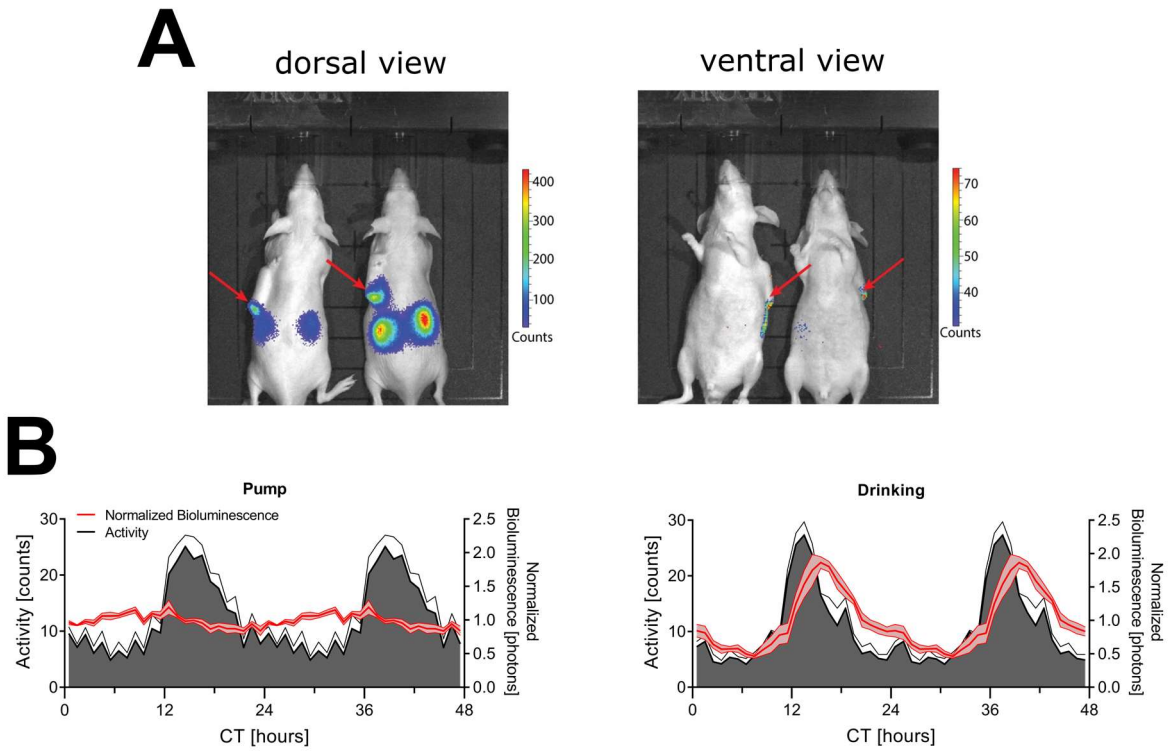


Supplementary Figure 2: **Sources of bioluminescence and different luciferin administration routes.** (A) Dorsal (left) and ventral (right) imaging of mice in IVIS Xenogen system. Note that the scale bar of the dorsal view has higher values than the scale bar of the ventral view. Images are taken between ZT6-8. The red arrows indicate the location of the osmotic minipump flow moderator. (B) Mice constitutively expressing under control of the synthetic CAG promoter luciferase received luciferin via an osmotic mini-pump (left) or in their drinking water (right) (n=4). Graphs are double plotted to aid visualization. CT = circadian time.

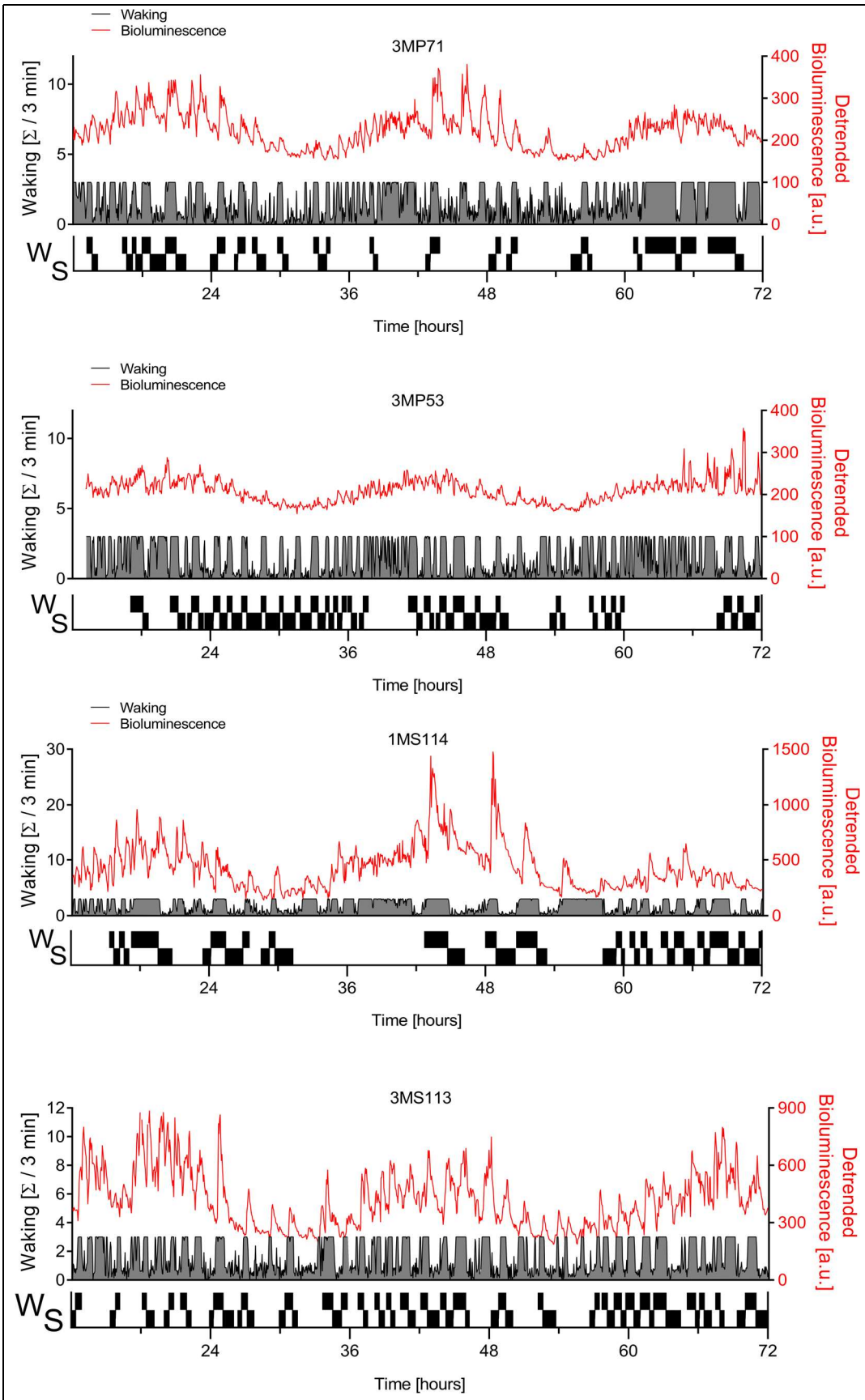


Supplementary Figure 3 (with Fig. 1B): **Bioluminescence co-detected with EEG-based sleep-wake state in the other four mice**. Legend as in Fig. 1B.

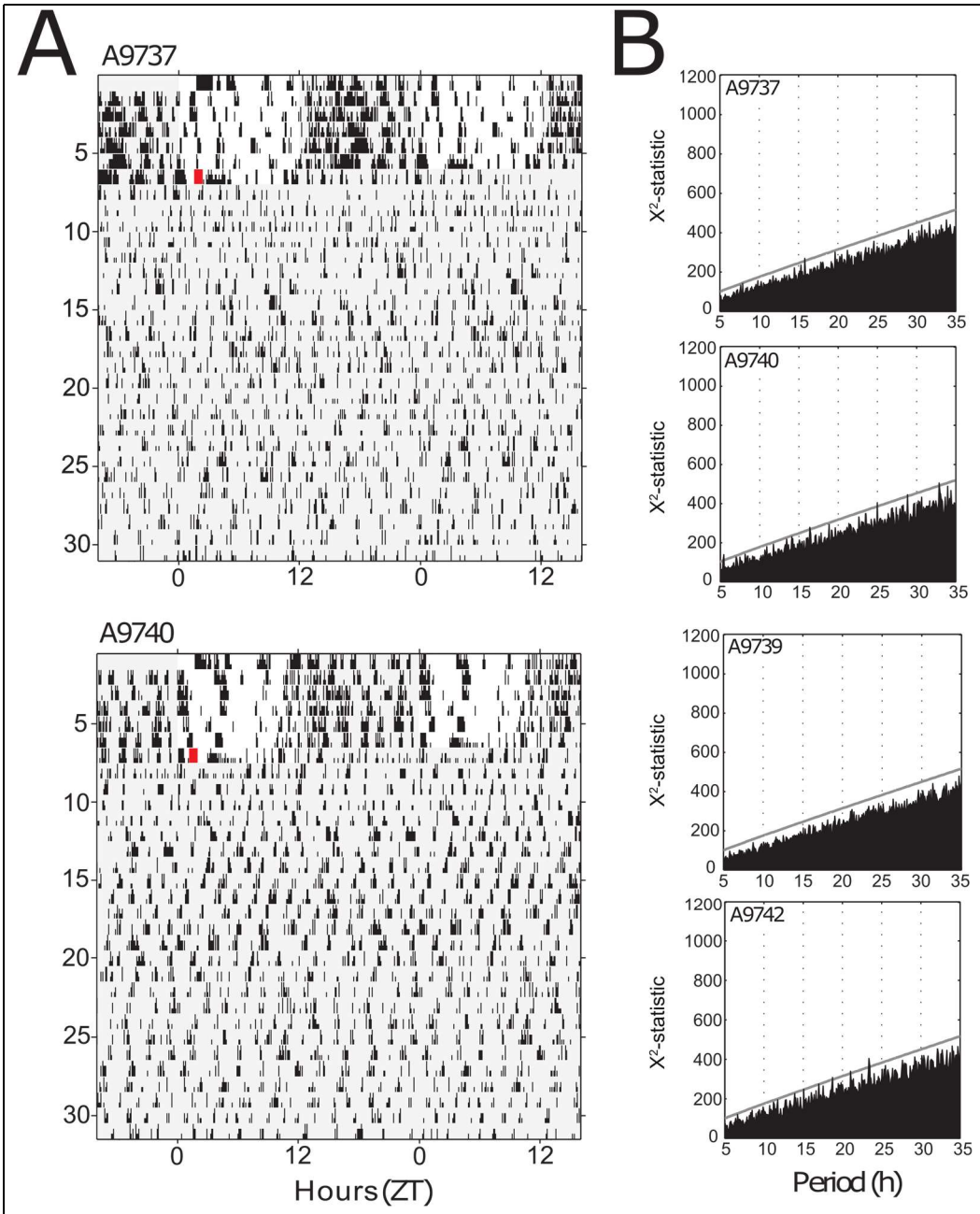


Supplementary Figure 4: **SCN-lesion eliminates circadian organization of locomotor activity**. (**A**) Examples of double-plotted actograms for two mice kept under LD12:12 condition (days 1-7 vertical axis) before bilateral lesion of the SCN (red square) and subsequently released under DD conditions (days 7-31). Light-grey areas denote darkness. (**B**) Chi-square periodograms of locomotor activity under DD following SCN lesion. Analysis in upper two graphs concern the mice illustrated in A. Grey lines in each panel indicate P=0.001 significance level.

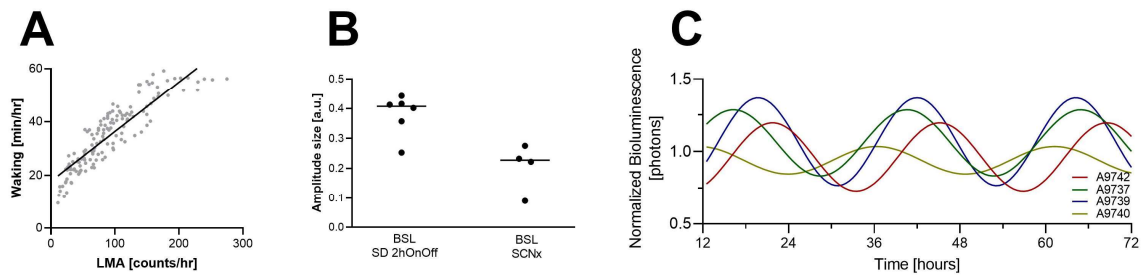


Supplementary Figure 5 (with Fig. 4): **Wake-to-LMA correlations and circadian amplitude estimation in baseline** (**A**) Locomotor activity (LMA) and waking measured in the 2hOnOff protocol EEG experiment, linear regression, $p<0.0001$, $R^2=0.79$. (**B**) Amplitude of PER2-bioluminescence observed during baseline. (**C**) Fitted sine-wave per individual for PER2 oscillation observed during baseline in SCNx mice. Average period was estimated at 23.7±0.6h (n=4). It should be noted that individual estimate errors were large (range 0.6-1.4h) due the shortness of the recording (~2.5 cycles).

730

731

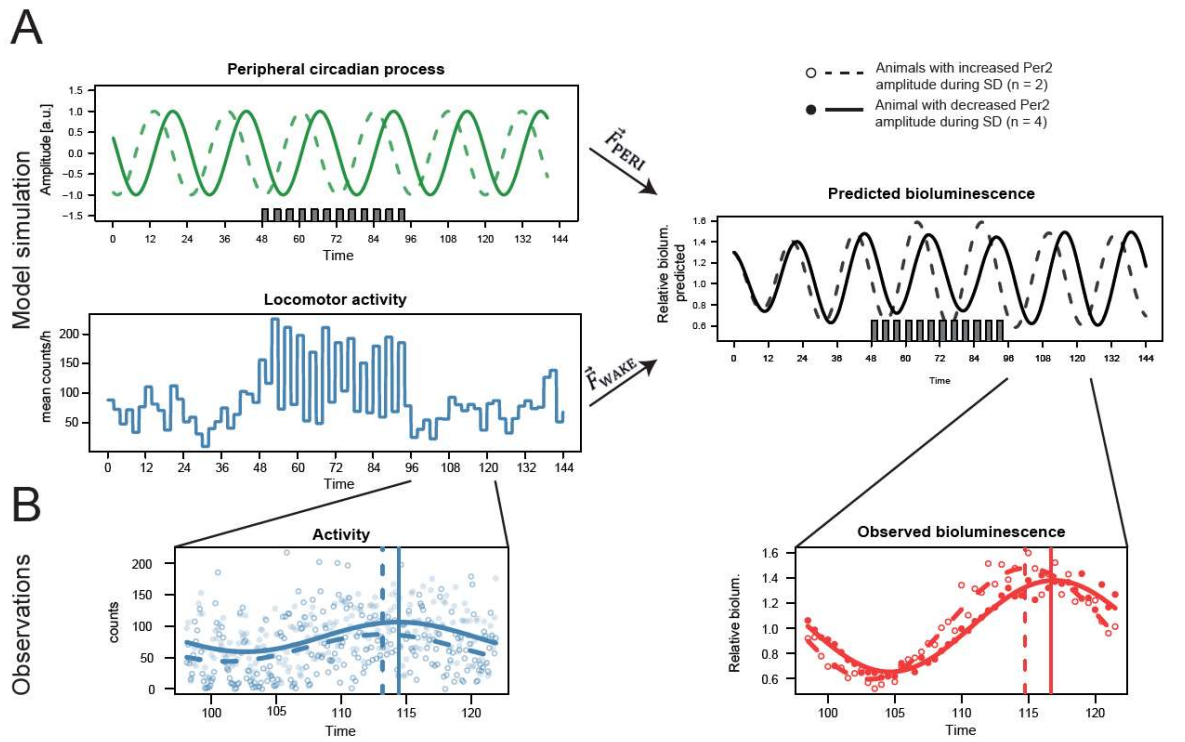


Supplementary Figure 6: **Can phase individual differences in $\vec{F}_{\mathrm{PERI}}$ phase explain individual differences in the change in the amplitude of the PER2 bioluminescence rhythm during the 2hOnOff protocol? (A)** Model simulation using fitted parameters as in Fig. 4C (solid lines) and assuming a 6h phase advance of $\vec{F}_{\mathrm{PERI}}$ dashed lines). Amplitude of predicted PER2 level (black lines) increased during 2hOnOff when phase was advanced (dashed), while it decreased using the fitted parameters (solid line). $\vec{F}_{\mathrm{PERI}}$ in green; $\vec{F}_{\mathrm{WAKE}}$ in blue. **(B)** Phase advance observed for PER2 bioluminescence (red) and wake (blue) in mice at the end of sleep deprivation for mice which increased PER2 bioluminescence amplitude during 2hOnOff (empty circles, n=2) vs those in which amplitude decreased (filled circles, n=4). Phase (vertical line) was calculated using sine-wave fitting (solid and dashed lines).

732

733 **References**


734 Akhtar, R. A., Reddy, A. B., Maywood, E. S., Clayton, J. D., King, V. M., Smith, A. G., Gant, T.
735 W., Hastings, M. H., & Kyriacou, C. P. (2002). Circadian Cycling of the Mouse Liver
736 Transcriptome, as Revealed by cDNA Microarray, Is Driven by the Suprachiasmatic Nucleus.
737 *Current Biology*, *12*(7), 540–550. https://doi.org/10.1016/S0960-9822(02)00759-5

738 Andrews, R. V. (1968). Temporal secretory responses of cultured hamster adrenals.
739 *Comparative Biochemistry and Physiology*, *26*(1), 179–193. https://doi.org/10.1016/0010-
740 406x(68)90324-1

741 Baker, F. C., Angara, C., Szymusiak, R., & McGinty, D. (2005). Persistence of sleep-
742 temperature coupling after suprachiasmatic nuclei lesions in rats. *American Journal of*
743 *Physiology. Regulatory, Integrative and Comparative Physiology*, *289*(3), R827-838.
744 https://doi.org/10.1152/ajpregu.00093.2005

745 Balsalobre, A., Brown, S. A., Marcacci, L., Tronche, F., Kellendonk, C., Reichardt, H. M.,
746 Schütz, G., & Schibler, U. (2000). Resetting of circadian time in peripheral tissues by
747 glucocorticoid signaling. *Science (New York, N.Y.)*, *289*(5488), 2344–2347.
748 https://doi.org/10.1126/science.289.5488.2344

749 Bass, J., & Takahashi, J. S. (2010). Circadian integration of metabolism and energetics.
750 *Science (New York, N.Y.)*, *330*(6009), 1349–1354. https://doi.org/10.1126/science.1195027

751 Cao, R., Gkogkas, C. G., de Zavalia, N., Blum, I. D., Yanagiya, A., Tsukumo, Y., Xu, H., Lee,
752 C., Storch, K.-F., Liu, A. C., Amir, S., & Sonenberg, N. (2015). Light-regulated translational
753 control of circadian behavior by eIF4E phosphorylation. *Nature Neuroscience*, *18*(6), 855–862.
754 https://doi.org/10.1038/nn.4010

755 Cao, Y.-A., Wagers, A. J., Beilhack, A., Dusich, J., Bachmann, M. H., Negrin, R. S., Weissman,
756 I. L., & Contag, C. H. (2004). Shifting foci of hematopoiesis during reconstitution from single
757 stem cells. *Proceedings of the National Academy of Sciences of the United States of America*,
758 *101*(1), 221–226. https://doi.org/10.1073/pnas.2637010100

759 Castelo-Szekely, V., Arpat, A. B., Janich, P., & Gatfield, D. (2017). Translational contributions
760 to tissue specificity in rhythmic and constitutive gene expression. *Genome Biology*, *18*(1), 116.
761 https://doi.org/10.1186/s13059-017-1222-2

762 Cederroth, C. R., Park, J.-S., Basinou, V., Weger, B. D., Tserga, E., Sarlus, H., Magnusson,
763 A. K., Kadri, N., Gachon, F., & Canlon, B. (2019). Circadian Regulation of Cochlear Sensitivity
764 to Noise by Circulating Glucocorticoids. *Current Biology: CB*, *29*(15), 2477-2487.e6.
765 https://doi.org/10.1016/j.cub.2019.06.057

766 Cheon, S., Park, N., Cho, S., & Kim, K. (2013). Glucocorticoid-mediated Period2 induction
767 delays the phase of circadian rhythm. *Nucleic Acids Research*, *41*(12), 6161–6174.
768 https://doi.org/10.1093/nar/gkt307

769 Cirelli, C., & Tononi, G. (2000). Differential expression of plasticity-related genes in waking and
770 sleep and their regulation by the noradrenergic system. *The Journal of Neuroscience: The*
771 *Official Journal of the Society for Neuroscience*, *20*(24), 9187–9194.

772 Cuesta, M., Cermakian, N., & Boivin, D. B. (2015). Glucocorticoids entrain molecular clock
773 components in human peripheral cells. *FASEB Journal: Official Publication of the Federation*
774 *of American Societies for Experimental Biology*, *29*(4), 1360–1370.
775 https://doi.org/10.1096/fj.14-265686

776 Curie, T., Maret, S., Emmenegger, Y., & Franken, P. (2015). In Vivo Imaging of the Central
777 and Peripheral Effects of Sleep Deprivation and Suprachiasmatic Nuclei Lesion on PERIOD-2
778 Protein in Mice. *Sleep*, *38*(9), 1381–1394. https://doi.org/10.5665/sleep.4974

779 Curie, T., Mongrain, V., Dorsaz, S., Mang, G. M., Emmenegger, Y., & Franken, P. (2013).
780 Homeostatic and circadian contribution to EEG and molecular state variables of sleep
781 regulation. *Sleep*, *36*(3), 311–323. https://doi.org/10.5665/sleep.2440

782 Daan, S., Beersma, D. G., & Borbély, A. A. (1984). Timing of human sleep: Recovery process
783 gated by a circadian pacemaker. *The American Journal of Physiology*, *246*(2 Pt 2), R161-183.
784 https://doi.org/10.1152/ajpregu.1984.246.2.R161

785 Damiola, F., Le Minh, N., Preitner, N., Kornmann, B., Fleury-Olela, F., & Schibler, U. (2000).
786 Restricted feeding uncouples circadian oscillators in peripheral tissues from the central
787 pacemaker in the suprachiasmatic nucleus. *Genes & Development*, 14(23), 2950–2961.
788 https://doi.org/10.1101/gad.183500

789 Dickmeis, T. (2009). Glucocorticoids and the circadian clock. *The Journal of Endocrinology*,
790 *200*(1), 3–22. https://doi.org/10.1677/JOE-08-0415

791 Edgar, D. M., Dement, W. C., & Fuller, C. A. (1993). Effect of SCN lesions on sleep in squirrel
792 monkeys: Evidence for opponent processes in sleep-wake regulation. *The Journal of*
793 *Neuroscience: The Official Journal of the Society for Neuroscience*, *13*(3), 1065–1079.

794 Engeland, W. C., Massman, L., Mishra, S., Yoder, J. M., Leng, S., Pignatti, E., Piper, M. E.,
795 Carlone, D. L., Breault, D. T., & Kofuji, P. (2018). The Adrenal Clock Prevents Aberrant Light-
796 Induced Alterations in Circadian Glucocorticoid Rhythms. *Endocrinology*, *159*(12), 3950–3964.
797 https://doi.org/10.1210/en.2018-00769

Franken, P. (2013). A role for clock genes in sleep homeostasis. *Current Opinion in Neurobiology*, *23*(5), 864–872. https://doi.org/10.1016/j.conb.2013.05.002

Franken, P., Dudley, C. A., Estill, S. J., Barakat, M., Thomason, R., O'Hara, B. F., & McKnight, S. L. (2006). NPAS2 as a transcriptional regulator of non-rapid eye movement sleep: Genotype and sex interactions. *Proceedings of the National Academy of Sciences of the United States of America*, *103*(18), 7118–7123. https://doi.org/10.1073/pnas.0602006103

Franken, P., Thomason, R., Heller, H. C., & O'Hara, B. F. (2007). A non-circadian role for clock-genes in sleep homeostasis: A strain comparison. *BMC Neuroscience*, *8*, 87. https://doi.org/10.1186/1471-2202-8-87

Gerber, A., Esnault, C., Aubert, G., Treisman, R., Pralong, F., & Schibler, U. (2013). Blood-borne circadian signal stimulates daily oscillations in actin dynamics and SRF activity. *Cell*, *152*(3), 492–503. https://doi.org/10.1016/j.cell.2012.12.027

Hastings, M. H., Maywood, E. S., & Brancaccio, M. (2018). Generation of circadian rhythms in the suprachiasmatic nucleus. *Nature Reviews. Neuroscience*, *19*(8), 453–469. https://doi.org/10.1038/s41583-018-0026-z

Hastings, M. H., Maywood, E. S., & Brancaccio, M. (2019). The Mammalian Circadian Timing System and the Suprachiasmatic Nucleus as Its Pacemaker. *Biology*, *8*(1). https://doi.org/10.3390/biology8010013

Hoekstra, M. M., Emmenegger, Y., Hubbard, J., & Franken, P. (2019). Cold-inducible RNA-binding protein (CIRBP) adjusts clock-gene expression and REM-sleep recovery following sleep deprivation. *ELife*, *8*. https://doi.org/10.7554/eLife.43400

Hor, C. N., Yeung, J., Jan, M., Emmenegger, Y., Hubbard, J., Xenarios, I., Naef, F., & Franken, P. (2019). Sleep–wake-driven and circadian contributions to daily rhythms in gene expression and chromatin accessibility in the murine cortex. *Proceedings of the National Academy of Sciences*, *116*(51), 25773–25783. https://doi.org/10.1073/pnas.1910590116

Kofuji, P., Mure, L. S., Massman, L. J., Purrier, N., Panda, S., & Engeland, W. C. (2016). Intrinsically Photosensitive Retinal Ganglion Cells (ipRGCs) Are Necessary for Light Entrainment of Peripheral Clocks. *PloS One*, *11*(12), e0168651. https://doi.org/10.1371/journal.pone.0168651

Kolbe, I., Husse, J., Salinas, G., Lingner, T., Astiz, M., & Oster, H. (2016). The SCN Clock Governs Circadian Transcription Rhythms in Murine Epididymal White Adipose Tissue. *Journal of Biological Rhythms*, *31*(6), 577–587. https://doi.org/10.1177/0748730416666170

830 Kornmann, B., Schaad, O., Bujard, H., Takahashi, J. S., & Schibler, U. (2007). System-driven
831 and oscillator-dependent circadian transcription in mice with a conditionally active liver clock.
832 *PLoS Biology*, *5*(2), e34. https://doi.org/10.1371/journal.pbio.0050034

833 Le Minh, N., Damiola, F., Tronche, F., Schütz, G., & Schibler, U. (2001). Glucocorticoid
834 hormones inhibit food-induced phase-shifting of peripheral circadian oscillators. *The EMBO*
835 *Journal*, *20*(24), 7128–7136. https://doi.org/10.1093/emboj/20.24.7128

836 Mang, G. M., & Franken, P. (2012). Sleep and EEG Phenotyping in Mice. *Current Protocols in*
837 *Mouse Biology*, *2*(1), 55–74. https://doi.org/10.1002/9780470942390.mo110126

838 Mang, G. M., & Franken, P. (2015). Genetic dissection of sleep homeostasis. *Current Topics*
839 *in Behavioral Neurosciences*, *25*, 25–63. https://doi.org/10.1007/7854_2013_270

840 Maret, S., Dorsaz, S., Gurcel, L., Pradervand, S., Petit, B., Pfister, C., Hagenbuchle, O.,
841 O'Hara, B. F., Franken, P., & Tafti, M. (2007). Homer1a is a core brain molecular correlate of
842 sleep loss. *Proceedings of the National Academy of Sciences of the United States of America*,
843 *104*(50), 20090–20095. https://doi.org/10.1073/pnas.0710131104

844 Möller-Levet, C. S., Archer, S. N., Bucca, G., Laing, E. E., Slak, A., Kabiljo, R., Lo, J. C. Y.,
845 Santhi, N., von Schantz, M., Smith, C. P., & Dijk, D.-J. (2013). Effects of insufficient sleep on
846 circadian rhythmicity and expression amplitude of the human blood transcriptome.
847 *Proceedings of the National Academy of Sciences of the United States of America*, *110*(12),
848 E1132-1141. https://doi.org/10.1073/pnas.1217154110

849 Mongrain, V., Hernandez, S. A., Pradervand, S., Dorsaz, S., Curie, T., Hagiwara, G., Gip, P.,
850 Heller, H. C., & Franken, P. (2010). Separating the contribution of glucocorticoids and
851 wakefulness to the molecular and electrophysiological correlates of sleep homeostasis. *Sleep*,
852 *33*(9), 1147–1157. https://doi.org/10.1093/sleep/33.9.1147

853 Moore, R. Y., & Eichler, V. B. (1972). Loss of a circadian adrenal corticosterone rhythm
854 following suprachiasmatic lesions in the rat. *Brain Research*, *42*(1), 201–206.
855 https://doi.org/10.1016/0006-8993(72)90054-6

856 Ohnishi, N., Tahara, Y., Kuriki, D., Haraguchi, A., & Shibata, S. (2014). Warm water bath
857 stimulates phase-shifts of the peripheral circadian clocks in PER2::LUCIFERASE mouse. *PloS*
858 *One*, *9*(6), e100272. https://doi.org/10.1371/journal.pone.0100272

859 Ono, D., Honma, K., & Honma, S. (2015). Circadian and ultradian rhythms of clock gene
860 expression in the suprachiasmatic nucleus of freely moving mice. *Scientific Reports*, *5*, 12310.
861 https://doi.org/10.1038/srep12310

Saini, C., Liani, A., Curie, T., Gos, P., Kreppel, F., Emmenegger, Y., Bonacina, L., Wolf, J.-P., Poget, Y.-A., Franken, P., & Schibler, U. (2013). Real-time recording of circadian liver gene expression in freely moving mice reveals the phase-setting behavior of hepatocyte clocks. *Genes & Development*, *27*(13), 1526–1536. https://doi.org/10.1101/gad.221374.113

Saini, Camille, Morf, J., Stratmann, M., Gos, P., & Schibler, U. (2012). Simulated body temperature rhythms reveal the phase-shifting behavior and plasticity of mammalian circadian oscillators. *Genes & Development*, *26*(6), 567–580. https://doi.org/10.1101/gad.183251.111

Satinoff, E., & Prosser, R. A. (1988). Suprachiasmatic nuclear lesions eliminate circadian rhythms of drinking and activity, but not of body temperature, in male rats. *Journal of Biological Rhythms*, *3*(1), 1–22. https://doi.org/10.1177/074873048800300101

Schibler, U., Gotic, I., Saini, C., Gos, P., Curie, T., Emmenegger, Y., Sinturel, F., Gosselin, P., Gerber, A., Fleury-Olela, F., Rando, G., Demarque, M., & Franken, P. (2015). Clock-Talk: Interactions between Central and Peripheral Circadian Oscillators in Mammals. *Cold Spring Harbor Symposia on Quantitative Biology*, *80*, 223–232. https://doi.org/10.1101/sqb.2015.80.027490

Segall, L. A., & Amir, S. (2010). Exogenous corticosterone induces the expression of the clock protein, PERIOD2, in the oval nucleus of the bed nucleus of the stria terminalis and the central nucleus of the amygdala of adrenalectomized and intact rats. *Journal of Molecular Neuroscience: MN*, *42*(2), 176–182. https://doi.org/10.1007/s12031-010-9375-4

So, A. Y.-L., Bernal, T. U., Pillsbury, M. L., Yamamoto, K. R., & Feldman, B. J. (2009). Glucocorticoid regulation of the circadian clock modulates glucose homeostasis. *Proceedings of the National Academy of Sciences of the United States of America*, *106*(41), 17582–17587. https://doi.org/10.1073/pnas.0909733106

Tahara, Y., Kuroda, H., Saito, K., Nakajima, Y., Kubo, Y., Ohnishi, N., Seo, Y., Otsuka, M., Fuse, Y., Ohura, Y., Komatsu, T., Moriya, Y., Okada, S., Furutani, N., Hirao, A., Horikawa, K., Kudo, T., & Shibata, S. (2012). In vivo monitoring of peripheral circadian clocks in the mouse. *Current Biology: CB*, *22*(11), 1029–1034. https://doi.org/10.1016/j.cub.2012.04.009

Tamaru, T., Hattori, M., Honda, K., Benjamin, I., Ozawa, T., & Takamatsu, K. (2011). Synchronization of circadian Per2 rhythms and HSF1-BMAL1:CLOCK interaction in mouse fibroblasts after short-term heat shock pulse. *PloS One*, *6*(9), e24521. https://doi.org/10.1371/journal.pone.0024521

Travnickova-Bendova, Z., Cermakian, N., Reppert, S. M., & Sassone-Corsi, P. (2002). Bimodal regulation of mPeriod promoters by CREB-dependent signaling and CLOCK/BMAL1 activity.

895 *Proceedings of the National Academy of Sciences of the United States of America*, *99*(11),
896 7728–7733. https://doi.org/10.1073/pnas.102075599

897 van der Vinne, V., Swoap, S. J., Vajtay, T. J., & Weaver, D. R. (2018). Desynchrony between
898 brain and peripheral clocks caused by CK1δ/ε disruption in GABA neurons does not lead to
899 adverse metabolic outcomes. *Proceedings of the National Academy of Sciences of the United*
900 *States of America*, *115*(10), E2437–E2446. https://doi.org/10.1073/pnas.1712324115

901 Vassalli, A., & Franken, P. (2017). Hypocretin (orexin) is critical in sustaining theta/gamma-
902 rich waking behaviors that drive sleep need. *Proceedings of the National Academy of Sciences*
903 *of the United States of America*, *114*(27), E5464–E5473.
904 https://doi.org/10.1073/pnas.1700983114

905 Wisor, J. P., O'Hara, B. F., Terao, A., Selby, C. P., Kilduff, T. S., Sancar, A., Edgar, D. M., &
906 Franken, P. (2002). A role for cryptochromes in sleep regulation. *BMC Neuroscience*, *3*, 20.
907 https://doi.org/10.1186/1471-2202-3-20

908 Wu, T., Ni, Y., Kato, H., & Fu, Z. (2010). Feeding-induced rapid resetting of the hepatic
909 circadian clock is associated with acute induction of Per2 and Dec1 transcription in rats.
910 *Chronobiology International*, *27*(1), 1–18. https://doi.org/10.3109/07420520903398625

911 Yan, L., & Silver, R. (2002). Differential induction and localization of mPer1 and mPer2 during
912 advancing and delaying phase shifts. *The European Journal of Neuroscience*, *16*(8), 1531–
913 1540. https://doi.org/10.1046/j.1460-9568.2002.02224.x

914 Yasenkov, R., & Deboer, T. (2010). Circadian regulation of sleep and the sleep EEG under
915 constant sleep pressure in the rat. *Sleep*, *33*(5), 631–641.
916 https://doi.org/10.1093/sleep/33.5.631

917 Yoo, S.-H., Yamazaki, S., Lowrey, P. L., Shimomura, K., Ko, C. H., Buhr, E. D., Siepka, S. M.,
918 Hong, H.-K., Oh, W. J., Yoo, O. J., Menaker, M., & Takahashi, J. S. (2004).
919 PERIOD2::LUCIFERASE real-time reporting of circadian dynamics reveals persistent
920 circadian oscillations in mouse peripheral tissues. *Proceedings of the National Academy of*
921 *Sciences*, *101*(15), 5339–5346. https://doi.org/10.1073/pnas.0308709101

922 Zhang, B., Gao, Y., Li, Y., Yang, J., & Zhao, H. (2016). Sleep Deprivation Influences Circadian
923 Gene Expression in the Lateral Habenula. *Behavioural Neurology*, *2016*, 7919534.
924 https://doi.org/10.1155/2016/7919534

925

926